NUCLEAR EXPERIMENTAL TECHNIQUES

Spectrometer with a Vertex Detector for Experiments at the IHEP Accelerator

V. V. Avdeichikov[a], A. N. Aleev[a], E. N. Ardashev[b], S. G. Basiladze[c], G. A. Bogdanova[c], A. M. Vishnevskaya[c], V. Yu. Volkov[c], A. P. Vorob'ev[b], A. G. Voronin[c], S. N. Golovnya[b], V. F. Golovkin[b], S. A. Gorokhov[b], Ya. V. Grishkevich[c], P. F. Ermolov[c†], E. G. Zverev[c], S. A. Zotkin[c], D. E. Karmanov[c], V. I. Kireev[a], E. S. Kokoulina[a], V. A. Kramarenko[c], A. Ya. Kutov[a], G. I. Lanshchikov[a†], A. K. Leflat[c], S. I. Lyutov[c], V. Kh. Malyaev[b], M. M. Merkin[c], G. Ya. Mitrofanov[b], V. V. Myalkovskii[a], V. A. Nikitin[a], V. S. Petrov[b], V. D. Peshekhonov[a], A. V. Pleskach[b], M. K. Polkovnikov[b], V. V. Popov[c], I. A. Rufanov[a], V. N. Ryadovikov[b], V. A. Sen'ko[b], M. M. Soldatov[b], L. A. Tikhonova[c], N. F. Furmanets[a], A. G. Kholodenko[b], Yu. P. Tsyupa[b], N. A. Shalanda[b], A. I. Yukaev[a], and V. I. Yakimchuk[b]

[a] *Joint Institute for Nuclear Research (JINR), ul. Joliot-Curie 6, Dubna, Moscow oblast, 141980 Russia*
[b] *Institute for High Energy Physics (IHEP), ul. Pobedy 1, Protvino, Moscow oblast, 142281 Russia*
[c] *Skobel'tsyn Institute of Nuclear Physics (SINP), Moscow State University, Moscow, 119992 Russia*
Received February 27, 2012

Abstract—The stages of development and the current status of the versatile "Spectrometer with a Vertex Detector" setup designed for physics experiments at the U-70 accelerator of the Institute for High Energy Physics (Protvino) is described. The main detectors of the setup are the vertex detector based on silicon microstrip detectors, the wide-aperture magnetic spectrometer based on multiwire proportional chambers, and the lead-glass hodoscope γ detector. In the setup, there is a fast two-level trigger system for selecting required particle interactions. The key characteristics of the setup systems are presented, and the physical results obtained on it are briefly listed.

INTRODUCTION

In 1984, three groups of physicists under the direction of P.F. Ermolov (SINP), A.M. Moiseev (IHEP), and I.M. Gramenitskii (JINR) and the electronic group headed by S.G. Basiladze (at that time, Research Computer Center, Moscow State University) submitted a project of an experiment aimed at measuring cross sections and studying the mechanisms of charmed particle production in hadron–hadron interactions at the U-70 accelerator of the IHEP (Protvino) using the "Spectrometer with a Vertex Detector" (SVD) hybrid-type setup [1]. This setup includes a precision vertex detector, a magnetic spectrometer, a hodoscope Cherenkov γ detector, and a trigger system.

Studying processes of charmed particle production using this technique was novel for the U-70 accelerator energies (as compared to [2–12]). It was expected that experimental results would provide information differing in a qualitative sense from the known data

and critical for understanding the mechanisms of charmed particle production.

This experiment has the name E-161 [13]. It had to be performed in two stages. The primary task of the experiment was to precisely measure the cross sections for inclusive processes of particle production with open charm in pp and $\pi^- p$ interactions at energies of 60−70 GeV, and to estimate their topological cross sections. In the case of confirmation of rather large cross sections for these processes at these energies, it was expected that the minimum energy, at which these measurements were feasible, would be determined. The next step in studying charmed particle production was considered to consist in investigating the mechanisms of charmed particle pair production.

A decision was made that the development of the setup would be divided into two stages corresponding to the stages of the E-161 experiment. In the first stage, the setup consisted of the precision vertex detector based on a fast-cycling liquid-hydrogen bubble chamber with a trigger system, the wide-aperture magnetic spectrometer based on proportional chambers, and the hodoscope Cherenkov γ detector based
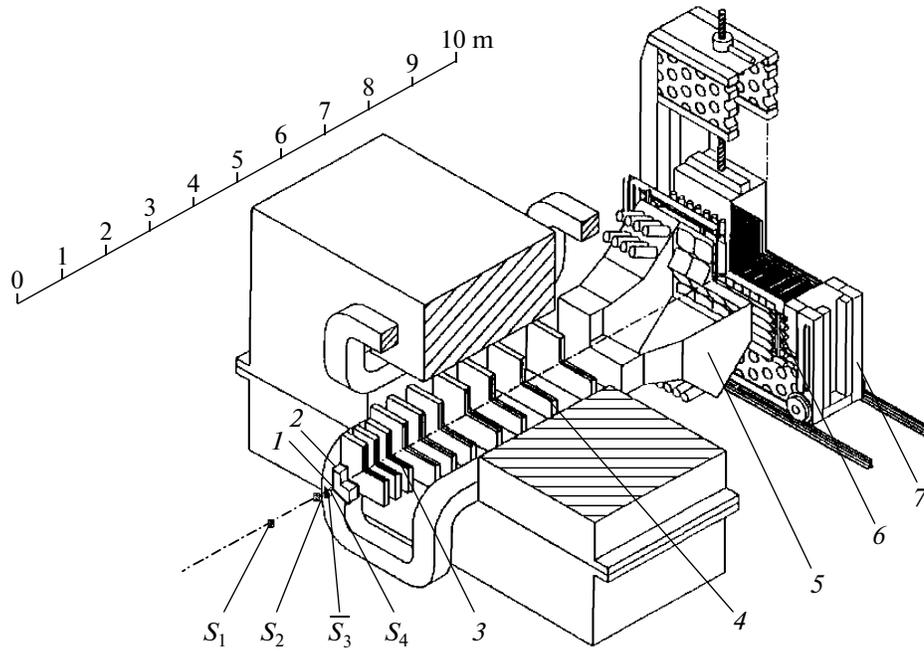
[†] Deceased.

Fig. 1. Detectors and a magnet of the SVD-2 setup: (*1*) fast-cycling bubble chamber (thereafter replaced with the active target), (*2*) precision vertex detector, (*3*) assembly of coordinate detectors ahead of the magnet (primarily, 1-m-long proportional chambers and, later, an assembly of mini-drift tubes), (*4*) magnetic spectrometer inside the magnet, (*5*) Cherenkov gas-filled detector, (*6*) scintillation hodoscope, (*7*) detector of γ quanta (DEGA), and (S_1, S_2, $\bar{S}_3$, S_4) scintillation detectors of the beam monitor.

on liquid glasses. At the second stage of setup development, it was expected that a substantial increase in the data acquisition rate (by a factor of 100 or more) would be achieved by designing a fast precision vertex detector based on an electronic technique, the spectrometer part would be upgraded, and additional detectors be included in the setup.

DETECTION AND DATA ACQUISITION SYSTEMS AT THE FIRST STAGE OF THE EXPERIMENT (SVD-1)

In this section, emphasis is placed on the detectors and the related systems, most of which, after several upgrades, have been used by now. The general view of the contemporary detectors in the SVD setup is shown in Fig. 1.

A Monitor, a Vertex Detector, and a Trigger System

Detection of short-lived charmed particles requires high precision in determining coordinates ($\sim 50-100$ μm) both of the primary interaction vertex and of the points of secondary activity due to charmed particle decay.

The vertex detector of the SVD-1 setup was a fast-cycling bubble chamber [14] in combination with microstrip silicon detectors (MSDs) (the strip pitch was 200 μm), the signals from which were used to monitor the beam and trigger of the setup. Information from the MSDs was also recorded on magnetic tape and used in geometrical reconstruction of events.

The arrangement of the detectors included in the beam monitoring system, the vertex detector, and the trigger system is shown in Fig. 2. Scintillation detectors S_1, S_2, and S_4 have dimensions of 80×80, 80×80, and 3×38 mm, respectively; detector $\bar{S}_3$ has a hole to let the beam pass through it. The beam propagates along axis Z; its cross section, which has an area of $\sim 2 \times 40$ mm^2, is stretched in the vertical direction along axis Y. Telescopes of multiwire proportional chambers (PCs) and MSDs are installed ahead of and past the target. The numbers of data readout channels are 128 for the MSD_{1Y}, 256 for the MSD_{2Y}, and 512 for the MSD_{2X} (896 channels in total). Detectors MSD_1 and MSD_2 are located at a distance of 25 cm from the target.

The electronics of the trigger subsystem was made to the CAMAC-COMPEX standard [15] on the basis of the nanosecond potential logic circuits [16]. It comprised the coincidence and veto modules, БР-214 register modules, special processors, INTEL 80386 universal microprocessor with a clock frequency of 33 MHz, and two Elektronika-85 personal computers. The multilevel trigger was intended to solve the following tasks: extracting a beam particle in the beamline by the coincidence of pulses from scintillation detectors S_1 and S_2 (signal *Monitor*), selecting interactions that happened in the effective target volume (the trigger of the second level), and enriching the experimental sample in events with charmed particle decays (the
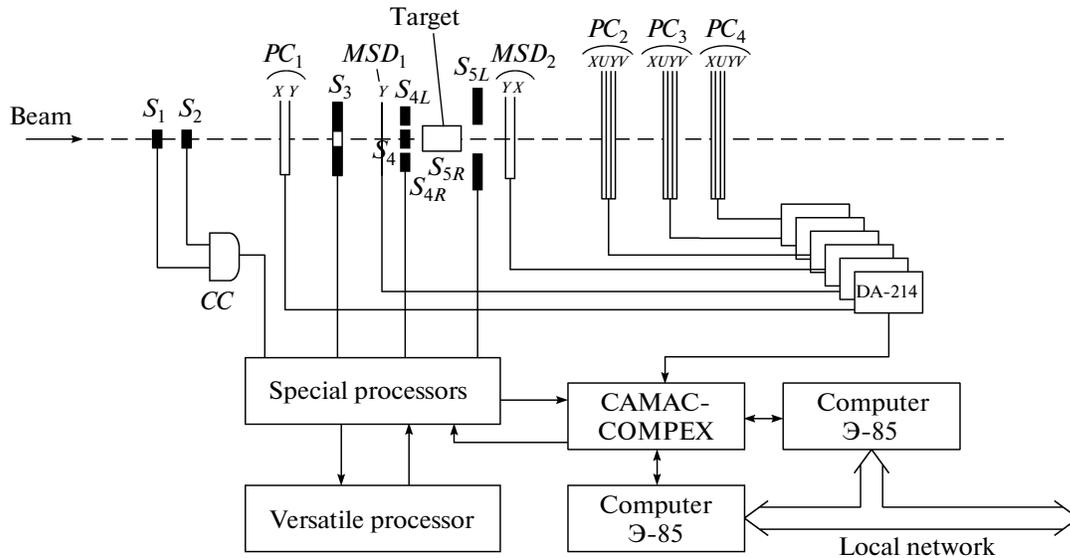
Fig. 2. Detector arrangement and block diagram of the equipment for event selection and data acquisition in the initial stage of the experiment: (S_1–S_5) scintillation detectors (S_3 has a hole to guide the beam), (S_{4L}, S_4, S_{4R}) three detectors placed in close contact with each other, (S_{5L}, S_{5R}) two detectors with a slit between them to guide the beam, (MSD) microstrip silicon detectors, (PC) proportional chambers (indices X, Y, U, and V label the wires (or strips) that have horizontal and vertical directions and form angles of ±10.5° with a vertical axis), (CC) coincidence circuit, and (DA) data acquisition module.

trigger of the third level). Both personal computers were used for prompt control of the equipment, data visualization, and control of the special processors and the trigger processor.

Magnetic Spectrometer

The wide-aperture magnetic spectrometer is an important part of the SVD setup. The PCs were initially grouped into ten units, three of which were installed in front of the magnet (later, they were replaced with a drift tube unit) and seven were placed into the MC-7A magnet (the length of the magnetic path downstream of the beam is 3 m; the aperture, i.e., width × height, is 1.8×1.2 m^2; and the field strength $B = 1.18$ T at a current of 4 kA). Each PC unit may contain two or three planes of wires located in the vertical (Y) or two inclined (U, V) directions. Depending on the chamber size, the number of wires in each plane may vary from 602 to 704. The total number of planes is 28, and the total number of signal wires is ~18 000.

Through the lack of free space in the magnet (the gap between the PCs and the magnet is 6 cm) only shaping amplifiers are fixed in place on the chambers, whereas the data acquisition electronics resides in the CAMAC crates situated in the experimental house. The length of the connecting cables is ~50 m. One crate contains data acquisition electronics for a single plane.

Signal readout from PCs. Readout and amplification of the signals from the signal wires are performed by shaping amplifiers of two types:

(i) 16-channel amplifiers produced by the Institute of Nuclear Physics (Siberian Branch, USSR Academy

of Sciences, Novosibirsk), which are based on a 155УД1 hybrid integrated circuit [17]; and

(ii) amplifiers based on a УИ5 hybrid integrated circuit produced by the Leningrad Institute of Nuclear Physics (Leningrad) [18].

The amplifiers of the first type have an input impedance of ~1 kΩ and a voltage gain of ~300. At their output, there is a common-emitter switch that has an adjustable threshold of action (from 300 to 700 mV) and provides a current of up to 30 mA; i.e., it is capable of forming transistor–transistor logic (TTL) voltage pulses in the output cable (a twisted pair with a wave impedance of ~110 Ω). To simplify the circuits, shaping of output pulses in duration has not been performed.

Practical experience shows that the high packaging density gives rise to a noticeable feedback effect of the output signal on the amplifier inputs, which makes the readout subsystem inclined to excitation if the number of channels is high. Therefore, the output current of the pulse shapers in the amplifiers has been reduced by about an order of magnitude, to the minimum level sufficient for triggering inputs of the TTL chips. To do this, common base transistors acting as impedance converters (from the wave impedance of the cable to ~1 kΩ) were placed at the outputs of the connecting cables.

In the amplifiers of the second type, the output current was limited by introducing an output current switch (~5 mA) as early as at the design stage.

Organization of the data acquisition modules. Each data acquisition crate contains the following modules:
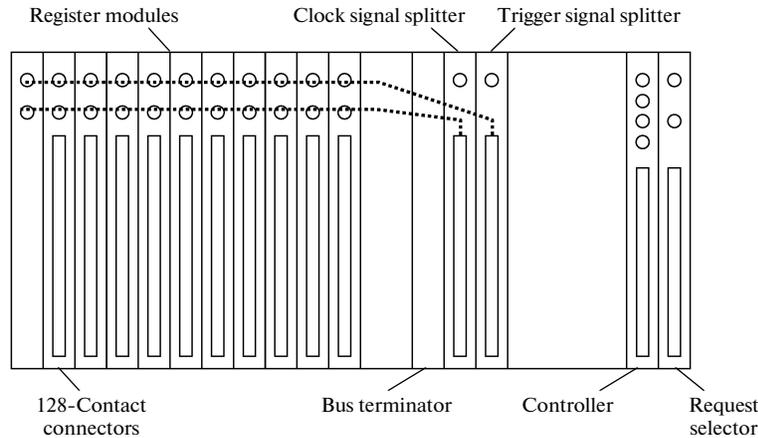
Fig. 3. Arrangement of the modules in the data acquisition crates of the magnetic spectrometer.

—РПК-213 64-channel modules for recording and encoding the signals from the PCs (one crate corresponds to a single PC);

—a КПК-671 crate controller [20], which outputs the signals to the intercrate bus that connects these crate controllers with the central crate;

—special TP-183 modules that split the clock and triggering signals; and

—С3-611 request selectors that filter out the register modules having no data prior to encoding.

Each module for recording the signals from the PCs has 64 inputs [19], and each crate contains 10 or 11 modules (Fig. 3). They are based on a fast memory (FM) for 16 64-bit words, which records the presence or absence of the signal in each of the module inputs in cycles recurring with a period of 80 ns (12 MHz). Since the FM has 16 address inputs, the total length of the time interval for storing data on the previous state of the inputs is ~1.2 μs. This time can be spent on generation of a triggering signal for the subsystem (the trigger of the first level) according to the required physical criteria.

The clock pulses are generated in the central control crate of the system and, thereafter, are distributed in two stages over all crates using the 16-channel NIM splitters. The centralized provision with clock pulses removes the problem of individual tuning that is characteristic of all systems with delay circuits in each data acquisition channel.

The triggering signal is distributed from the central crate among all register modules through identical splitters (see Fig. 3). Upon arrival of the triggering signal front, the FM in each module is switched from the data recording mode to the readout mode. For an event of particle passage near the signal wire to be extracted (at the instant of selected interaction), the following operations must be done:

(1) going back in time for the number of clock periods equal to the trigger system delay;

(2) in each channel, extracting an event of the pulse's arrival from the amplifier within the analyzed clock period; in other words, one must make sure that

(i) the state of the FM input was zero in the previous clock period, and

(ii) the state of the output changed from zero to unity in the clock period under investigation or in the next clock period (two periods are needed, since a pulse may be "cut off" and lost in a single clock period);

(3) generating the code of the triggered channel.

Since the physical processes being investigated on the SVD setup are characterized by a high multiplicity of secondary particles, there is a high probability that many signals will appear in the register module upon a single interaction. Therefore, each register module must have an internal stack memory (LIFO) for storing several codes of the triggered channels.

In the described system, the stack length allows simultaneous testing of all channels. In the case of binary coding, the above operations must be repeated 64 times, which takes much time. Moreover, the total code length obtained thereby will be rather large (64 6-bit codes). It is expedient that 64 inputs in the register module be divided into groups with 8 channels in each, the data be presented within the group in their initial linear code (i.e., in the form of an 8-bit set), and only the group number be represented in a binary code (3 bits). One can easily see that the maximum length of the code in this case is 88 bits (eight 11-bit codes) instead of 384 bits.

Four clock periods are needed to perform the above operations (1–3) within groups (the fourth period is used to store the group code in the stack). These operations are repeated eight times in all register modules and in all crates at once. Simultaneously with the coding, "zero" groups (containing no triggered channel) are filtered out. A total of 32 clock intervals are needed for coding all signals, which takes <6 μs.

The coding process is controlled by crate controllers [20]. In response to the trigger signal, they generate eight sets, each containing four pulses shifted in time with respect to each other. If even one triggered group is registered in the register module, this module produces the service request at the end of the control set of clock pulses. From this instant of time, the system is ready for data readout. Generally, data may not be read out if the second-level trigger system outputs the negative decision, i.e., rejects an event selected by the first-level trigger system.

Central system crate. The main modules of the central crate (Fig. 4) are as follows:

—KKC-731 branch crate controllers [21];

—a КЦК central crate controller [22] (with its own С3-611 request selector [23]), which connects the equipment with the online computer;

—a program-controlled delay unit (2БЗУ-122 [24], the range is 64 ns) for measuring delayed coincidence curves of the PCs;

—two pairs of special TP-183 modules for splitting the clock pulses and triggering pulses of the first level;

—a trigger signal generator (simulator; the left-hand Clock-730A module);

—a generator (simulator) of acceleration cycle start signals (the right-hand Clock-730A module);

—the INTERRUPT module of the synchronization system [25]; and

—two 214-БР-16 input registers of this subsystem, which assume the number of each next event from the setup trigger system.

The auxiliary crate contains the doubled 2СС-1511 coincidence circuit, which allows one to set operating conditions of the magnetic spectrometer. This system is operable in three modes:

(1) testing in the common SVD program;

(2) testing in a special control program; and

(3) operating mode in the common program.

Organization of data readout. CAMAC crates are used in the system design; however, the COMPEX protocol [15] is implemented on the crate bus in the readout system. The address space of this protocol is 24 bits, which corresponds to the modern standards (lines W_1-W_{24} are used). To increase the physical operating speed of the bus, load resistances of the bus lines are reduced down to 500 Ω (to do this, special modules—terminators—have been produced), and transceivers with high output currents are used in the register modules and the controllers. These measures have made it possible to shorten the cycle duration in the bus to 600 ns, i.e., almost by half as compared to the CAMAC bus cycle.

The readout system in the magnetic spectrometer is centralized (Fig. 5) and has, as is the case with CAMAC, three hierarchy level. The choice of the centralized structure is explained by the similarity of the majority of detectors, the simplicity of data coding algorithms admitting the centralized control, and the

requirement that data must be acquired in a single common memory. The use of the COMPEX protocol has made it possible to unify the layout of buses in the data acquisition crates, (cable) branches, and the central crate (as a matter of fact, the COMPEX protocol implies that the protocol of the CAMAC branch bus is transferred to the crate buses). There are four branches in total, each with its own interface controller [21] in the central crate (see Fig. 4). Each branch has seven data acquisition crates. An IBM personal computer is connected online to the central crate via its own interface controller [22]. This crate also contains modules for communication with the trigger system.

If the central crate receives a negative decision from the trigger subsystem of the second level, the computer produces reset signal Z in the bus of the central crate. This signal is distributed among all system crates via branch buses and, then, arrives at all register modules. If the decision is positive, the readout process starts. Since one crate corresponds to a single coordinate plane, the probability that each crate of the system being triggered will contain some data (for reading) is rather high. For this reason, data are read out in the simplest way, namely, by sequential by-turn interrogation (over the "program channel"). The central computer reads data out of each crate as long as there is an acknowledgment of the presence of data—Q in the readout cycle; afterward, it changes over to readout of the next crate.

Within the crate, reading proceeds as follows. As noted above, if a data acquisition module contains some data, it produces service request signal L. In the 25th crate station, there is a request selector [23] with a priority encoder (into a binary code); the priority represents the position of the module in the crate. The code of the current (highest-priority) request is transmitted by the selector over the auxiliary bus [15] to the crate controller. Upon receiving the read command from the computer, the controller uses this code for reading available data out of the register module (as many times as there are words in the stack). If data in the register module are exhausted, it removes signal L, and, in the next cycle, interrogation of the next-priority (next-position) register module starts. As a result, no additional program operations are required for finding the encoded data at the crate level (this is done by hardware), and data readout proceeds at the highest rate possible for this equipment.

The factor determining the readout rate is the physical operating speed of the branch bus; the readout cycle for one coordinate takes ~4.5 μs. A total of ~300 words are read in an event; i.e., the read time for a single event is ~1.2 ms. Therefore, data from ~750 events can be received over 1 s of beam extraction from the accelerator (~10^6 particles).

System monitoring firmware. A control system has been developed for the spectrometer. It allows testing of the operability of individual channels, modules, crates, and the system as a unit in the absence of the
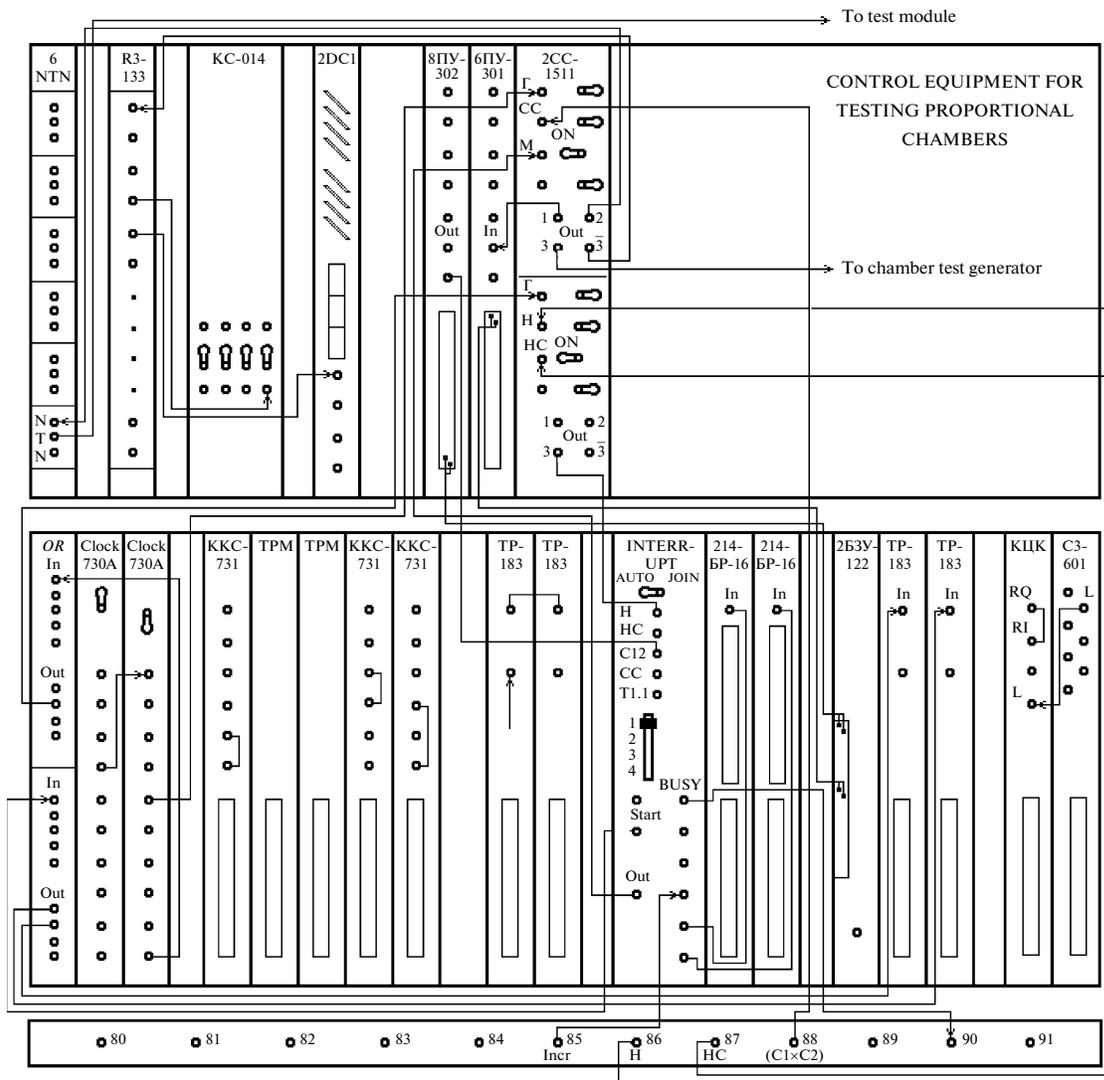
Fig. 4. Central and auxiliary crates of the magnetic spectrometer electronics with the cable panel of the synchronization system shown at the bottom: (6NTN) NIM−TTL−NIM level converter, (R3-133) NIM signal splitter, (KC-014, 2DC1) pulse counters, (6ПУ-301, 8ПУ-302) NIM−ECL−NIM level converters, (2CC1) dual coincidence circuit, (*OR*) NIM signal combiner, (Clock-730A) TTL (frequency) generators, (KKC-731) (inter)crate communication controller, (TPM, TP-183) multichannel splitters−generators of the clock pulses, (2БЗУ) controlled nanosecond delay unit, (КЦК) central crate controller, and (C3-611) selector of requests (LAM) of the crate modules.

accelerator beam. The monitoring system is based on a pulse generator the signal from which can be applied to any cathode plane of PCs via a mechanical switch. The presence of parasitic capacitances "cathode plane−anode wire" causes the generator signal to be divided among all channels, owing to which the performance of each wire in each chamber, can be checked.

The second important module of the monitoring subsystem is the program-controlled delay module [24] with a 1-ns step and a range of 128 ns, which allows the trigger pulse to be shifted in time with respect to the wire signals.

The special program written in the 'C Builder' language using graphical tools is the software component of the monitoring system. This program performs the following operations:

(1) testing the serviceability of the central system crate;

(2) testing each data acquisition crate in each branch;

(3) checking each wire in each plane by collecting and analyzing histograms from the test generator;

(4) plotting the delayed coincidence curves for each plane in the testing and operating modes (on the beam), which helps select the optimal trigger signal delay time.

Our magnetic spectrometer is one of the largest instruments of this type in Russia. For many years, it has been used to good effect at the U-70 accelerator,
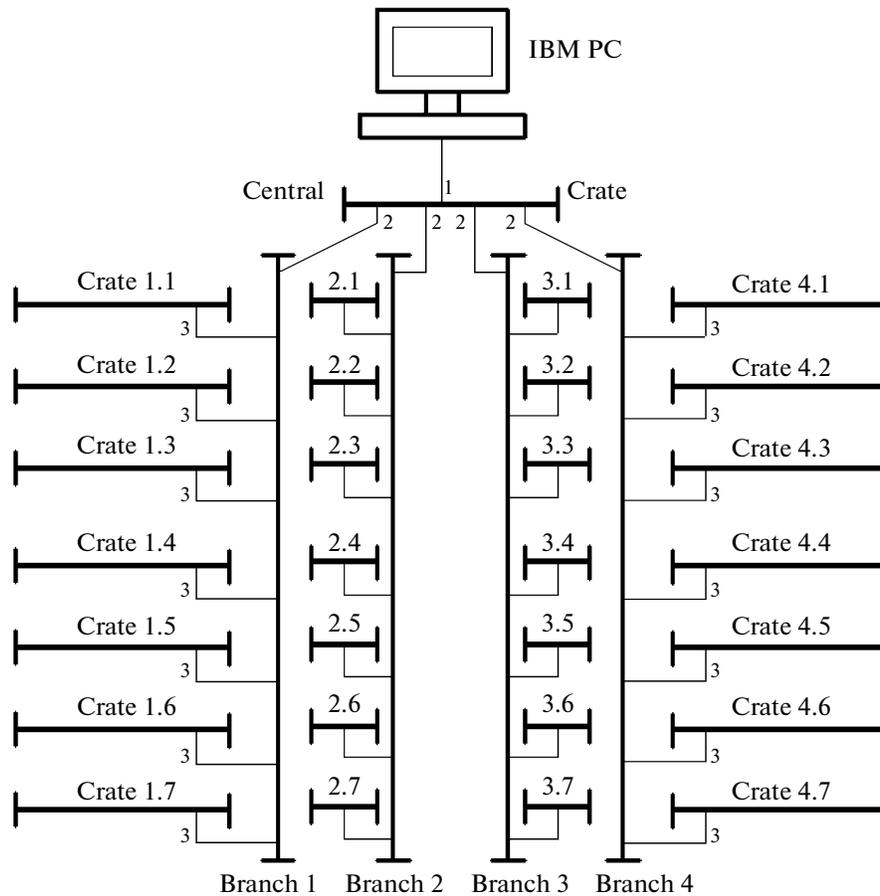
Fig. 5. Layout of buses for the data taking system of the magnetic spectrometer. Interface controller: (1) IBM controller, (2) branch controller, and (3) crate controller.

and the fraction of the experiment time lost for failures in its equipment was always very small.

Two runs of measurements in the proton beam with a momentum of 70 GeV/c were performed at the SVD-1 setup in 1992 and 1994, in which ~310000 frames were recorded (about 20% of the expected statistics), with track densities of 100–300 bubbles/cm at a bubble diameter of 25–30 μm. As is the case with all hybrid setups combining the chamber-based and electronic techniques, processing of experimental data was performed in two steps. The first step implied processing of photographic frames from the fast bubble chamber, and the second consisted in joining information obtained thereby with the data from the magnetic spectrometer. The preliminary results obtained at the first stage of the experiment were reported at the XXVII International Conference on High Energy Physics [26]. The cross sections for charmed particle production in pp interactions at 70 GeV/c were preliminarily estimated [27, 28]. Nevertheless, the low efficiency in detection and reconstruction of rare processes on the setup built in the first stage of the experiment has required an essential increase in the operating speed of the setup and its substantial upgrading.

Proposal for the Second Stage of the Experiment

In 1998−1999, the staff members at the SINP (Moscow), IHEP (Protvino), JINR (Dubna), and the Institute for High Energy Physics, Tbilisi State University (Tbilisi, Georgia) submitted a proposal for SVD upgrading [29]. In the second stage, the experiment was aimed at studying the mechanisms of charmed particle production in pA interactions at 70 GeV and their decays, and received the name E-184.

Main objectives of the second stage of the experiment. Acquisition of a vast body of data on decays of charmed particles offers a chance to carry out the following investigations:

(1) measuring the total cross section of charmed particle production in nuclear interactions with a precision of 10% or better (the required statistics is ~300 decays);

(2) measuring the A dependence of the total cross section from data obtained on Si nuclei and other targets (the required statistics is 500 decays for each target);

(3) measuring the differential cross section in the Feynman variables and transverse momentum p_T and studying the leading effect (the required statistics is 1000 decays for each target);

(4) searching for effects associated with the mechanism of hidden charm release (the required statistics is 2500−3000 decays for each target);

(5) testing the applicability of the quantum chromodynamics perturbation theory to describe the near-threshold charmed particle production and verifying the predictions of the two-component models [30, 31] (the required statistics is 2500−3000 decays for each target); and

(6) determining the modes of little-studied Λ_c^+-baryon decays (the required statistics is 2500−3000 decays for each target).

Required composition of the setup for the second stage of the experiment. For the above-stated problems to be solved, the experimental setup must provide a means for reconstructing the kinematical characteristics of charmed particles over a wide range of variables x_F (the Feynman variable) and p_T.

Both the wide-aperture magnetic spectrometer with PCs and the γ detector based on total-absorption Cherenkov counters, which had been produced in the first stage of the experiment, were included in the SVD-2 setup without substantial changes. Scintillation detectors of the beam monitoring system, small PCs for beam diagnostics, and a large scintillation hodoscope located in front of the γ detector were also produced and adjusted in this stage of the experiment.

It was also necessary that the following detectors be developed for this stage:

—a fast precision vertex detector based on microstrip silicon detectors;

—an array of six planes of mini-drift tubes; and

—a detector identifying the sort of particles based on a threshold cellular Cherenkov counter.

In addition, the trigger system electronics had to be renewed, and a system for data acquisition and representation be developed on the basis of the novel (at that time) fast network communication facilities and new computers.

DETECTION AND DATA ACQUISITION SYSTEMS IN THE SECOND STAGE OF THE EXPERIMENT (SVD-2)

Considerable progress in studying charmed particles on extracted beams has been achieved in recent years owing to the development of the technique of precision vertex detectors (PVDs) based on the electronic method and the use of powerful processors capable of promptly processing a large body of experimental data. The PVD technique allows one to rapidly estimate the shift of secondary tracks with respect to the primary vertex in order to select events with decays of short-lived particles on the real-time basis of the experiment, as well as to reconstruct the vertices of these decays. In addition, targets with various atomic numbers can be easily included into the PVD.

Complex PVDs containing many MSDs with several tens of thousands channels were used in the experiment of the next generation aimed at studying photo- and hadron-production of heavy quarks on the extracted beams at CERN and FNAL [32−34]. The quantity of reconstructed decays of charmed particles was as many as 10^5, which offered a chance to proceed to comprehensive investigation of the hadroproduction dynamics of charmed quarks and the mechanisms of their decay.

Since the shift value $\delta \approx c\tau$ is practically independent of the momentum of a decaying charmed particle [35], the PVD technique can be profitably used to improve the signal-to-noise ratio in investigations of charmed particles in the near-threshold region. Therefore, it was proposed using a fast PVD with a structure optimized for the energy range under investigation to perform the second stage of the study of charmed particle production. The expected PVD functions are as follows:

—at the level of online event selection, the coordinates of the interaction point and the coordinates on the trajectories of primary and secondary charged particles must be measured with accuracies of ±150 and ±5 μm, respectively, which allow one to establish the fact of primary particle interaction inside the target and the presence of secondary vertices adjacent to the primary one;

—at the level of geometrical track reconstruction, readings of the PVD detectors must guarantee a high (~3 mrad) two-track resolution for charged particles emitted at small angles, and allow high-efficiency reconstruction of the trajectories of all charged particles; and,

—at the level of event topology reconstruction, data obtained using the PVD must allow reconstruction of secondary vertices located at a distance of 5 mm from the primary interaction point and association of third-level tracks to them.

A Vertex Microstrip Detector

The design, the parameters of the vertex detector sensors, and the signal readout electronics were described in [36]. Figure 6 presents the schematic diagram of the vertex detector structure [37]. The detector includes the following parts:

(1) the beam telescope, which has been designed to detect the passage of initial beam particles (protons) from the accelerator and determine their direction and is composed of three pairs of sensors (MS_1-MS_6) providing a full interception of a ~3-mm-diameter beam area;

(2) active (i.e., sensitive to tracks) target *AT*, in which protons in proton−nucleus interactions initiate primary interactions; a small portion of the latter (~10^{-4}) contains charged particles or rare events with
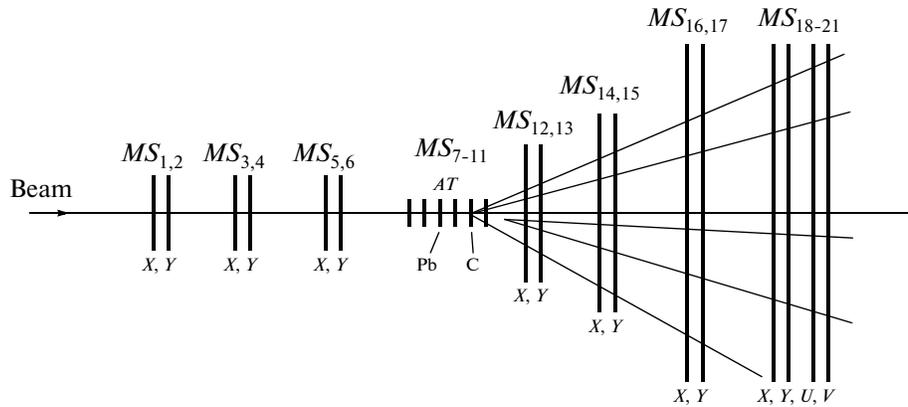
Fig. 6. Composition of the vertex detector components: (MS_1-MS_6) beam telescope sensors, (MS_7-MS_{11}) target sensors, ($MS_{12}-MS_{17}$) vertex telescope sensors, ($MS_{18}-MS_{21}$) tracking system sensors, and (AT) active target.

a high hadron multiplicity, as well as narrow hadron resonances;

(3) the main (tracking) part of the vertex detector, which is used to record tracks, select primary and secondary vertices and is composed of five (X, Y) pairs of sensors for measuring tracks within a polar-angle aperture θ of ±250 mrad and an azimuthal angle φ of $0-360°$, where θ is the angle of the secondary tracks with respect to the direction of the initial beam track, and φ is the initial angle in the plane of protons; this aperture is comparable to the aperture of the other detectors in the setup.

The sensors are produced from 100-mm silicon plates. The dimensions of the sensors and their relative position on the Z axis are presented in the table (the coordinate of the first sensor in the active target is assumed to be $Z = 0$).

Active target. To permit the solving of physical problems using the vertex detector, the target must perform the following functions:

—extracting events with the primary interaction inside the target at the stage of the first-level trigger signal generation;

—preliminarily localizing the vertex of an event by the Z and $X(Y)$ coordinates, which is used thereafter to produce the trigger of the second level and in the subsequent geometrical reconstruction of the event; and

—providing a means for investigating the A dependence of the charmed particle production mechanism by setting supplementary passive layers between its active layers, so that the substances of these layers differ widely in atomic number (light carbon C and heavy lead Pb).

The overall view of the target is shown in Fig. 7 [38]. The target consists of a set of strip silicon sensors MS_7-MS_{11} and is mounted at the center of the fiberglass laminate printed circuit board shaped as a disk with a thickness of 1.5 mm, a diameter of 200 mm, and a hole at its center 30 mm in diameter. Preamplifiers (a total of 48 preamplifiers) are also mounted on the

board. The length of the commutating conductors connecting the target strips with the preamplifier inputs is <30 mm.

The target is shaped as a cylinder. The cylinder walls are formed by Plexiglas rings assembled into a package. The bottom and cap of the cylinder are produced from an aluminum foil 20 μm thick. The target is assembled immediately on the printed circuit board and is positioned with reference to the central hole. When in operation, the target is oriented so that the cylinder axis is aligned with the primary beam direction. A printed circuit board with a silicon detector fixed in place on it is inserted and tightened between each pair of rings. The board is made from aluminized polyimide; the thicknesses of the bearing polyimide layer and the printed aluminum conductors are 10 and 20 μm, respectively (see Fig. 7, on the right). The board is automatically tightened in the radial direction during target assembling due to the conical profile formed by the joined rings in the package. The tension factor of the board in the radial direction is 0.04 the inner radius of the ring. A silicon sensor is welded to the aluminum conductors at the center of each board. The sensor crystal is fixed in place on the board only by its symmetrical welding.

Readout and data acquisition electronics. The vertex detector comprises amplifying multichannel integrated circuits of two types:

—Gassiplex chips [39] (16 channels, 10 MHz), which amplify the signals from the sensors of beam telescope MS_1-MS_6 and vertex telescope $MS_{12}-MS_{17}$ (Fig. 8, on the left); and

—Viking chips [40] (128 channels, 10 MHz), which amplify the signals from sensors $MS_{18}-MS_{21}$ of the tracking system (Fig. 8, on the right).

In view of the short pulse shaping time (~0.5 μs), integrated circuits of the first type are used to organize the trigger system of the second level for selection of charmed particles, whereas chips of the second type are used to simplify the vertex detector design. The

Table

Sensor number and strip orientation	Purpose	Strip position	Active area of the sensor, mm	Z coordinate, mm	Strip separation, mm
1, 2 (X, Y)	Beam telescope	Vert., horiz.	16 × 16	−1000; −1000	25
3, 4 (X, Y)		Vert., horiz.		−500; −500	25
5, 6 (X, Y)		Vert., horiz.		−12; −11	25
7−11 (Y)	Active target	Vertical	8 × 8	0, +4, +12* +18, +22	1000
12, 13 (X, Y)	Detector tracker	Vert., horiz.	16 × 16	+31; +32	25
14, 15 (X, Y)		Vert., horiz.	32 × 32	+51; +52	50
16, 17 (X, Y)		Vert., horiz.	51 × 51	+81; +82	50
18, 19 (X, Y)		Vert., horiz.	51 × 51	+106; +113	50
20, 21 (U, V)		Tilt 10.5°	51 × 51	+120; +126	50

* To study the dependence of the cross sections on the atomic number of the nucleus, a passive target—a lead foil 220 μm thick—is located at a point with Z coordinate of +8 mm, and the passive target—a carbon plate 500 μm thick—is located at a point with Z coordinate of +16 mm.

total number of channels for signal amplification and shaping is ~10 000.

Vertex detector software. Three high-speed computers are included in the vertex detector (IBM Pentium III 800 MHz and higher), of which

—two are intended for the vertex detector: they simultaneously record data from the vertex telescope and the tracker system to ensure the required operating speed of the vertex detector;

—the third is the central computer used to receive and analyze information from the entire system and, in addition, to control the other detectors of the setup in which the vertex detector is included.

The computers of the subsystem (except for the magnetic spectrometer) operate on the Windows 98 platform, and the computer of the magnetic spectrometer and the central computer operate under Windows XP. The programming language of the software is C++ in the Borland Builder v6.0 and Borland C++ v5.02 integrated shells. All programs are equipped with a convenient user interface, state-of-the-art visualization tools, and graphics.

The software developed for the vertex detector includes the following parts:

—tests for the CAMAC crate−computer communication modules;

—tests for the synchronization modules;

—tests for the electronic modules of the vertex detector with the simulation of its performance from the testing signals;

—software for doing methodological works; and

—program package for taking data from the vertex detector.

The program package for data acquisition is used to perform the following functions:

(1) taking calibration measurements and calculating the calibration constants both upon manual triggering and in the automatic mode; calibration results are saved for each plane to the file of pedestals; general results of the calibration are available in the *svd.log* file and can be visualized on the histograms of planes;

(2) loading the calibration constants into the amplitude analysis modules (AAM, AAB, and AAT-N);

(3) "compiling" data using the КОМП modules and data filtering circuits of the AAT-N modules;

(4) taking data from all operable channels (~10 000) in the mode of "zero" channel exclusion with a rate of ~1000 events/s;

(5) creating, filling, and visualizing histograms to control the quality of data (mean amplitudes, signal spectra from selected channels and integrally from the whole detector);

(6) operation of the synchronization circuit from direct passing particles and the trigger of the first level in the automatic mode and jointly with the other subsystems of the setup;

(7) saving and storing physical information on the hard disk in the automatic mode; and

(8) transmitting data and controlling jobs using the TCP/IP protocol in case of joint operation.

The vertex detector and the readout electronics were tested as parts of the other equipment of the SVD-2 setup on the ITEP accelerator beam. The following characteristics have been obtained:

—fraction of inoperative and noisy channels, 5% (of 9200);

—error of coordinate measurements:

in sensors with a pitch of 25 μm, 5 μm;

in sensors with a pitch of 50 μm, 10 μm;

—error in measuring angles, 0.2 mrad;

—detection efficiency for tracks, 96%;

—track multiplicity recording, >40 tracks.

These characteristics correspond to the world-class level of vertex detector parameters.
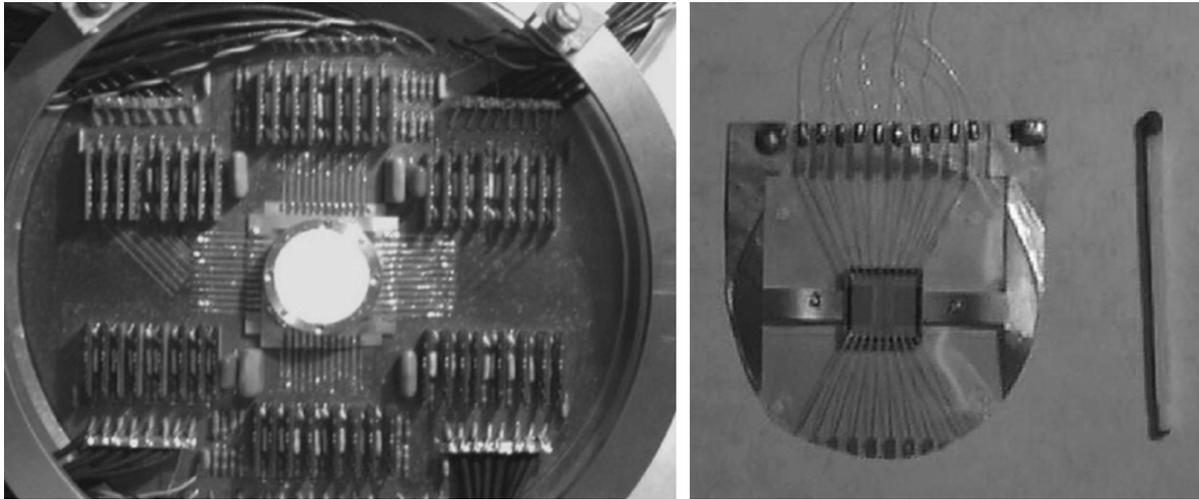
Fig. 7. External appearance of the target (left) mounted on the printed circuit board (at the center); the target is surrounded by six groups of preamplifiers with eight preamplifiers in each group; and mount of the silicon detector (right).
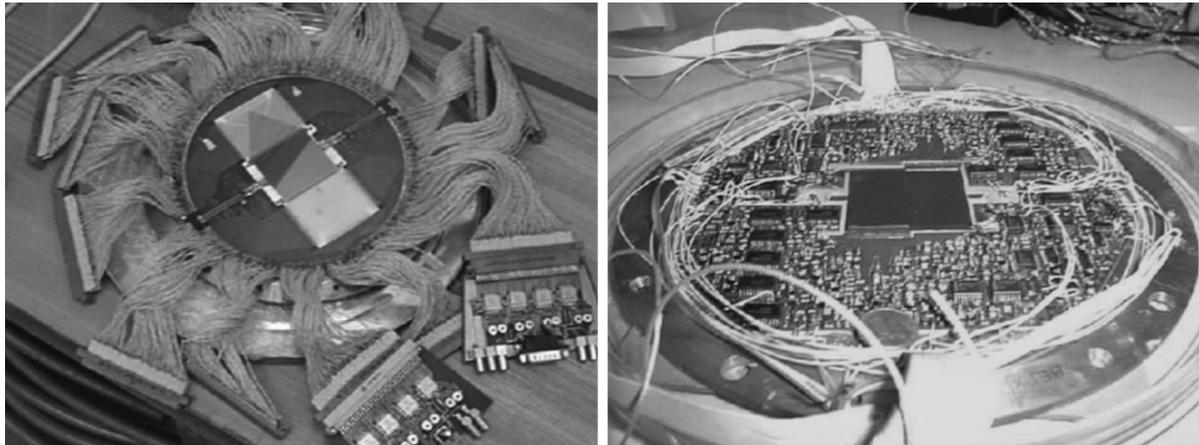

Fig. 8. Microstrip detectors with the Gassiplex (left) and Viking chips (right).

It is possible to receive the following bodies of data over 1 s of beam extraction: 750 events/s from the Gassiplex with 300 words in an event and 1000 events/s from the Viking with 150 words in an event.

An Assembly of Mini-drift Tubes

To join particle tracks in the PVD and tracks recorded in the proportional chambers of the magnetic spectrometer and improve the measurement accuracy to ~0.3 mm, the 1-m-long proportional chambers were replaced with a unit of mini-drift tubes, which is a system of cylindrical (made of a current-conducting film) gas-filled detectors combined into three double-layer planar modules.

The design of the drift tubes and the related electronics are described below in the Section "Thermalization Project at the SVD-2 Setup."

Threshold Cherenkov Detector

A multichannel threshold gas-filled Cherenkov detector placed between magnet MC-7 and the scintillation hodoscope is used for charged particle identification. This detector consists of two 3-m-long sections with an entrance aperture of 177×130 cm². In the back part of the detector, there are rectangular spherical mirrors with dimensions of 42×33 cm and radius of curvature $R = 200$ cm, arranged into four horizontal rows, with eight mirrors in each row. The total area covered by the mirrors is 265×155 cm² in projection onto the plane perpendicular to the counter axis. The detector volume is viewed by 32 ФЭУ-125 photomultiplier tubes (PMTs) with a cathode diameter of 140 mm, which are supplemented with Winston light collectors. There is a fast preamplifier near the voltage divider of the PMT. The signal from the preamplifier is transmitted over the coaxial cable
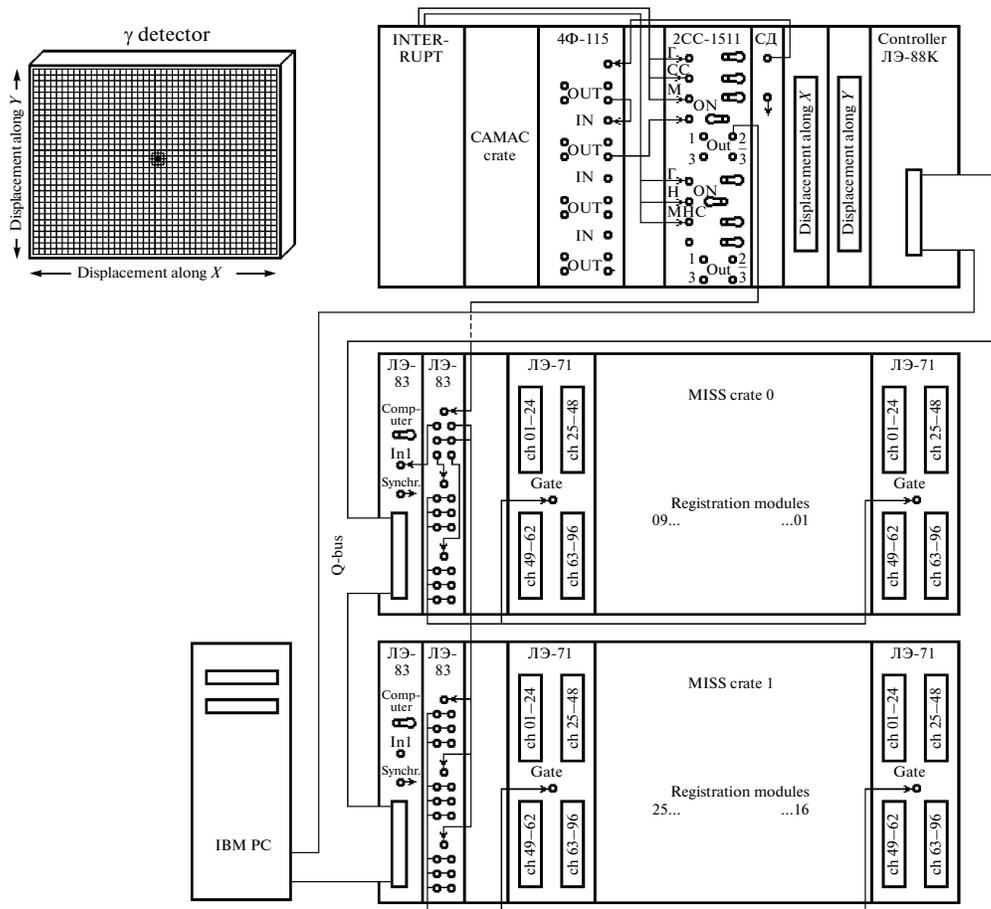
Fig. 9. Block diagram of the equipment for recording signals from the γ detector.

through the delay line to the analog-to-digital converter (ADC) from which it is read out by the crate controller into the local computer.

The detector filled with Freon at atmospheric pressure and a temperature of 20°C is capable of identifying pions in the momentum range from 6 to 21 GeV/c with an efficiency of 98%, which allows, for 50% of events, reliable discrimination between D^0 and $\overline{D}^0$ mesons detected by the spectrometer.

Scintillation Hodoscope

The scintillation hodoscope is installed on a movable platform of the γ detector at a distance of ~8.3 m from the target and is composed of two planes of scintillation detectors (H_L and H_V) oriented vertically and horizontally. In each horizontal plane, there are 12 detectors with scintillators produced by the extrusion method with hot molding of the light guide at its end. The operating field of the scintillator is 200×2400 mm at a thickness of 10 mm. In the vertical plane, there are 12 detectors with the operating field of the scintillator of 200×1400 mm.

Physically, the hodoscope detectors are self-contained and light-proofed; each detector comprises a ФЭУ-110 PMT with a high-current voltage divider and is equipped with a monitoring system of a driver and an optical fiber. The hodoscope is mounted on a frame, which is fixed in place on the γ detector truss.

The data acquisition electronics of the scintillation hodoscope contains 36 signal shapers and 36 channels of gated registers, and the event selection logic comprises 5 multi-input coincidence circuits.

γ Detector

The DEGA hodoscope γ detector with lead glass radiators is used to detect π^0 mesons and γ quanta from charmed particle decays. The DEGA is located at a distance of ~8.9 m from the active target. This detector consists of $32 \times 48 - 4 = 1532$ (in the earlier modification, $32 \times 42 - 4 = 1340$) total-absorption Cherenkov counters with glasses having transverse dimensions of 38×38 mm^2 and a length of 505 mm and coupled to ФЭУ-84-3 PMTs. The total cross sectional area of the detector is ~1.9×1.3 m^2 (earlier, ~1.6×1.3 m^2). Physically, the DEGA is a self-contained detector and is
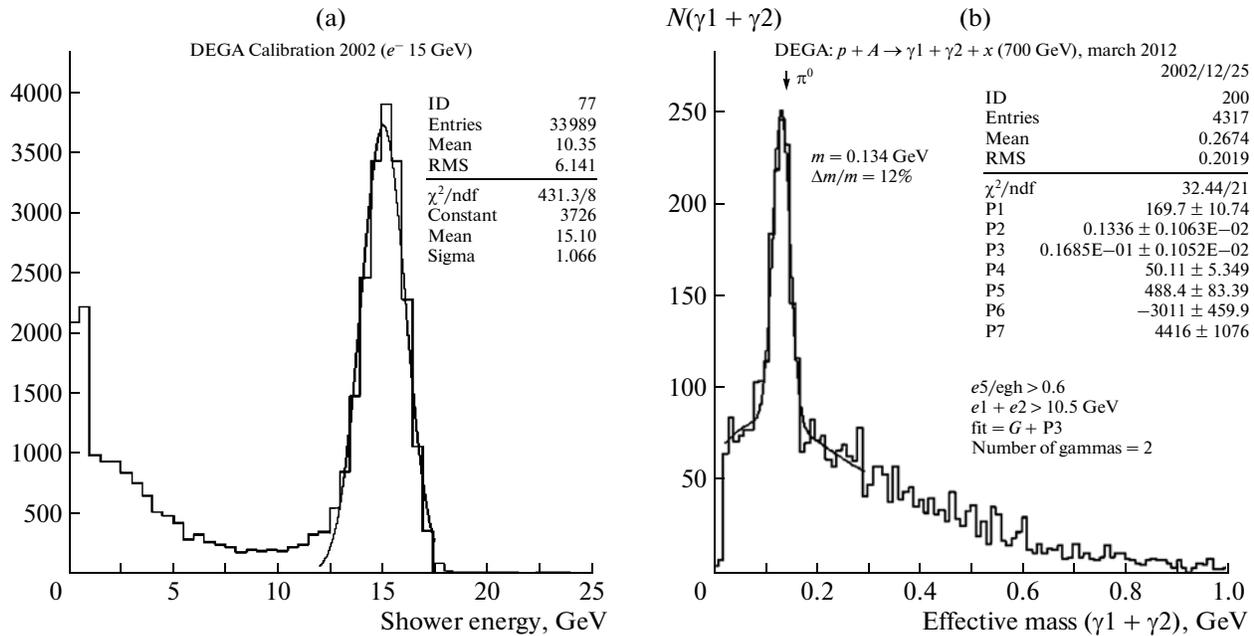
Fig. 10. (a) Total signal of the electron avalanche in the DEGA at an electron energy of 15 GeV, and (b) effective mass spectrum of two showers, provided that their total energy is >10 GeV.

installed at a distance of 3 m behind the MC-7 magnet on a platform capable of moving under remote control along two axes perpendicularly to the beam. The DEGA detects γ quanta in a momentum range from 300 MeV/c to 20 GeV/c with a coordinate accuracy of 2−3 mm. The geometrical detection efficiency for single π^0 mesons from decays of Δ_c^+ and D escaping in the center-of-mass system in the forward hemisphere ranges from 20 to 30%.

Data acquisition electronics for the DEGA. Initially, the DEGA electronics included Le Croy 2282 charge-to-digital converters [41]. Today, the electronics has been upgraded for the E-190 experiment (see Section "Thermalization Project") and is based on 96-channel QDC-96 charge-to-digital converters included as components in the MISS system developed by the IHEP [42].

The schematic diagram of the γ detector and its electronics are presented in Fig. 9 on a scale of about 1 : 100. The electronic equipment contains two MISS crates for recording PMT signals and one CAMAC crate for generating the *Gate* signals for the charge-to-digital converters and synchronizing their operation with the other components of the setup [43]. The MISS crates comprise the following modules:

—96-channel ЛЭ-71 signal register modules;

—ЛЭ-83 crate controllers connected to the Q bus that links them with the IBM computer;

—ЛЭ-67 standard MISS splitters of the logical (NIM) signals.

During calibration, the DEGA was exposed to a narrow (3 mm in diameter) electron beam (E = 15 GeV),

which sequentially irradiated the center of each counter. The movement of the mobile system along transverse axes X and Y was controlled by two CAMAC modules located in the upper crate (see Fig. 9).

The total signal of an electron avalanche in the DEGA was obtained at an electron energy of 15 GeV using the equalizing coefficient (Fig. 10a). The energy resolution of the DEGA is seen to be 1/15 (6.7%). The signal from neutron pions was also extracted when the spectrometer with the vertex detector was exposed to a 70-GeV proton beam. Figure 10b shows the spectrum of the effective masses of two showers under the condition that their total energy is >10 GeV.

TRIGGER AND SYNCHRONIZATION SYSTEMS OF THE SVD-2 SETUP IN THE E-184 EXPERIMENT

Trigger System in the E-184 Experiment

The trigger selected for the E-184 experiment extracts interactions in the active target and is based on fast estimation of the signal amplitudes from the MSDs of the active target [44]. This estimate also provides a means for determining the Z coordinate of the interaction point. The active target used in the setup was composed of five silicon plates with an area of 8 × 8 mm and a thickness of 300 μm, which are segmented into eight 1-mm-wide strips. The target detectors had a low (<1 μA) dark current and were grouped according to the full depletion voltage, which was ~50 V. The breakdown voltage of the target detectors exceeded 200 V [43]. A 240-μm-thick lead foil was
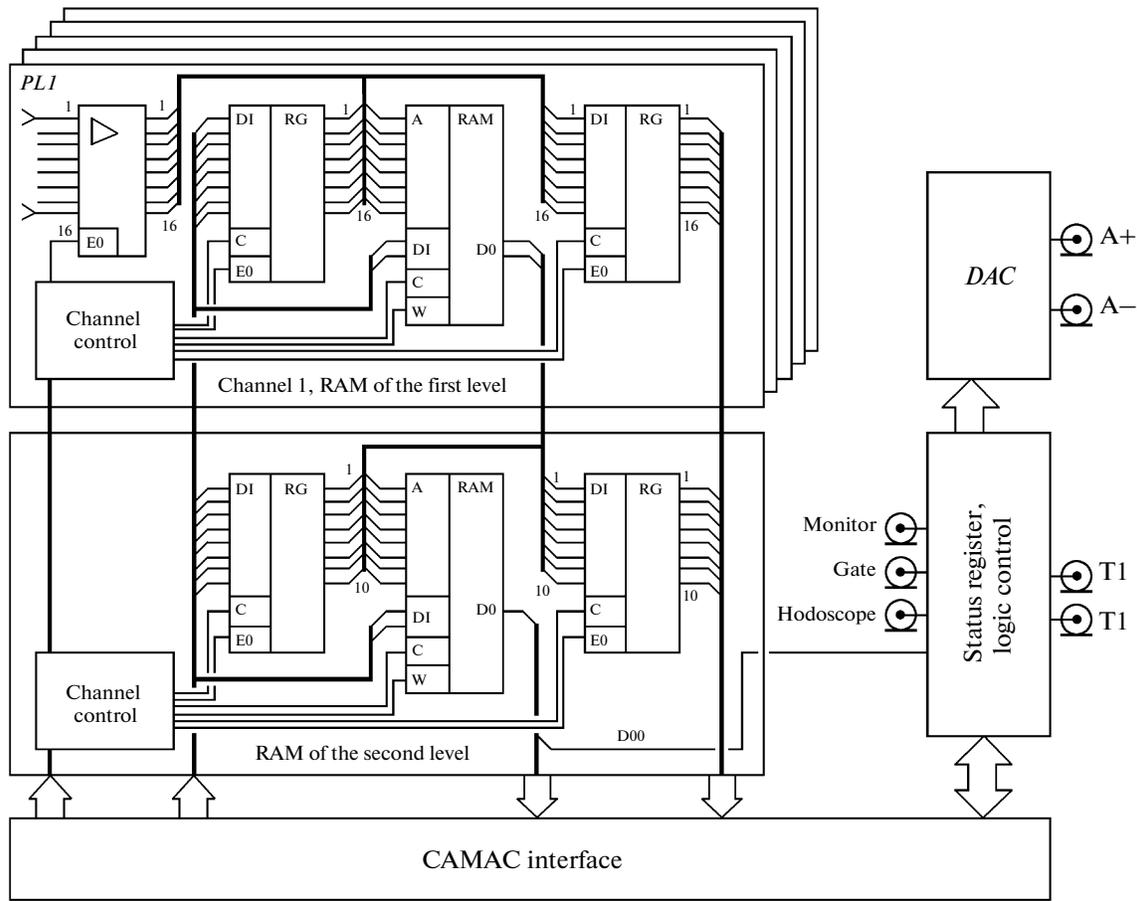
Fig. 11. Functional diagram of the trigger system of the setup.

inserted between the second and third target layers, and a 520-μm-thick carbon plate was inserted between the third and fourth layers. The step in mounting of all target planes was 4 mm downstream of the beam. The detectors of the active target, as well as all MSDs of the setup, were produced by the Research Institute of Material Science and Technology (Zelenograd, Moscow) and passed certification on the complex of the testing equipment for measuring the MSD parameters [45, 46].

The calculations in [47] show that it is possible to perform fast selection of events having a secondary particle with high p_T if secondary particles are detected in strips of the scintillation hodoscope located at some distance from the beam axis. This will allow extraction of events with $(c, \bar{n})$ pairs as early as at the first trigger level.

To start operation of the Spectro local system, the trigger signal must arrive at it no later than 700 ns after the hit of the beam particle. To start the Vertex local system, the key elements of which are Gassiplex amplifiers, the trigger signal must arrive within 400–

500 ns after the interaction in the active target. The time interval from the instant of particle passage through the active target to the arrival of the trigger signal at the DEGA local system must not exceed 400 ns. This is the most critical operating condition of the trigger system.

Trigger System Electronics

The functional diagram of the trigger system is presented in Fig. 11. The modules included in this system are described below.

Active target analyzer (ATA) is intended for amplification and amplitude discrimination of signals arriving from intermediate amplifiers *IA*. The module contains eight amplitude discrimination channels, six digital-to-analog converters (DACs) for specifying thresholds, and eight DACs for restoring the base line and testing the module.

Positive polarity signals arrive at the inputs of each channel and, without being amplified and inverted,

Fig. 12. Functional diagram of the TPM-2 module: (*PL*) programmable logics.

are fed to three comparators that specify three amplitude discrimination levels. The other inputs of the comparators receive the threshold voltages from the DAC chips. The threshold DACs are grouped so that one DAC serves one of the three thresholds for four of the eight channels. If a signal exceeds the threshold, the comparator outputs a positive voltage step, which charges the capacitor that sets a delay time of ~100 ns. This is done for a case when the input signals arrive slightly earlier than the trigger signal.

Within 20 ns after the trigger signal arrival, the data from the comparators are fed to the priority encoder and written into the output data registers. Within 40 ns after the trigger signal arrival, the data are ready and are available at the module output for 200 ns. As a result, the module produces a 16-bit word (with two bits per channel) containing the code of the amplitude.

The RGH module (the hodoscope register) is a 16-bit module designed to record the signals from the scintillation hodoscope and prepare data for the T-HOD (the hodoscope trigger) module. The RGH module is also used in the data acquisition system of the Cherenkov detector. The module has a 16-channel input, an L-port for the gate signal for writing, the L-port for the

fast reset, and a 16-channel inverting output. Writing by the gate pulse from the front panel is organized so that both the leading edge and the pulse amplitude from the input will be written into the register over the whole duration of the write gate pulse. Output data from the module are not gated. To test the trigger electronics, it is possible to write data into the register from the CAMAC bus.

The TPM-2 module (the target trigger) is used to make a decision on the presence of inelastic interaction of a primary particle in five active segmented planes and two passive planes of the target. The functional diagram of the module is shown in Fig. 12.

The module is organized as a two-level random-access memory (RAM) in which the output data of the first level are the address for the second. A CY7C192-25 static memory integrated circuit (IC) with 16 address inputs and 4 separated data inputs/outputs is used. The module starts operating upon arrival of the start signal from the front panel. The pulse leading edge sets the start flip-flop, forming an internal RAM access signal. This signal arrives at the enable inputs of the incoming buffers, as well as at the RAM inputs *Package selection*.
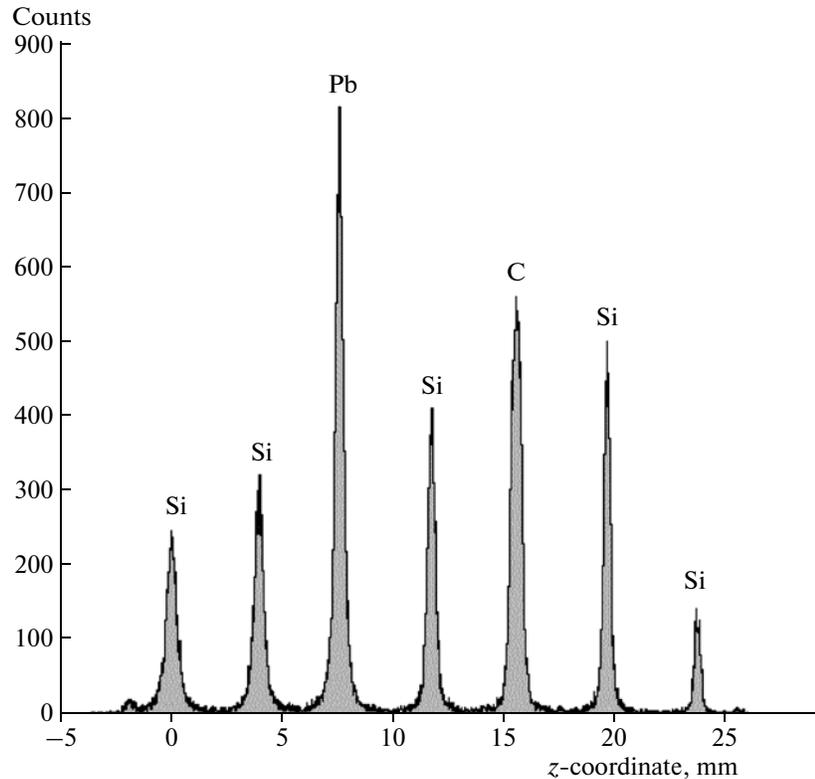
Fig. 13. Spatial distribution of the interaction vertices along the Z axis in the active target.

Data from five 16-bit inputs arrive at address inputs of the first-level RAM, which operates as $16 \rightarrow 2$ (it produces a two-bit word of output data based on the 16-bit input address), and data from their outputs are fed to the address inputs of the second-level RAM, which operates as $10 \rightarrow 1$. The data from the second-level RAM output go to the coincidence circuit, which also receives the status signals from the scintillation hodoscope. All these signals are recorded into a status register in response to the trailing edge of the start trigger signal. The signal from the output of the coincidence circuit is formed by duration (50 ns) and arrives at the outputs of the module. The total delay of the module for outputting the first-level trigger signal is 100 ns or less. An 8-bit DAC is embedded into the module; it is used for end-to-end testing of the AAM, ADC, and TPM-2.

The T-HOD module (the hodoscope trigger) has been built for making a decision on the presence of secondary particles in the scintillation hodoscope and is capable of converting any combination of input bits. The circuit diagram of this module is simpler relative to the TPM-2 module. It constitutes two single-level RAMs operating according to the scheme $16 \rightarrow 1$, the output signals from which can be separately delivered to the front panel or combined by the logical pulse *AND/OR*. A similar static memory CY7C192-25 is used. The module has two 16-bit address inputs, the

inputs of the start of conversion and "latching" the result, as well as outputs of the ready decision.

Logic scheme of the trigger system. The signals from the scintillation detector (see Fig. 11) are shaped by their amplitude and duration and fed to the TPC coincidence–anticoincidence module. Its output pulse arrives at the SYNCHRON-2 module, which produces a signal that acts as a gate signal for the AAM and RGH modules and a start signal for the TPM-2 and T-HOG modules. At the same time, the scintillation hodoscope signals are independently shaped by their length and recorded into registers of the RGH module. The signals from 16-bit outputs of the RGH module are sent to the inputs of the T-HOD module, where they are subjected to one-level table conversion. The output signal of the T-HOD module, arriving at the input of the module, can be derived from any combination of input signals.

To generate trigger signal *T1*, the signals from the segments of the target detectors is amplified by fast low-noise amplifiers and transmitted over coaxial cables to two groups of modules. Each of the three modules of the first group—ADCs—has 16 channels of 12-bit analog-to-digital conversion. Five modules of the second group—AAM—each have eight channels of three-level discrimination.

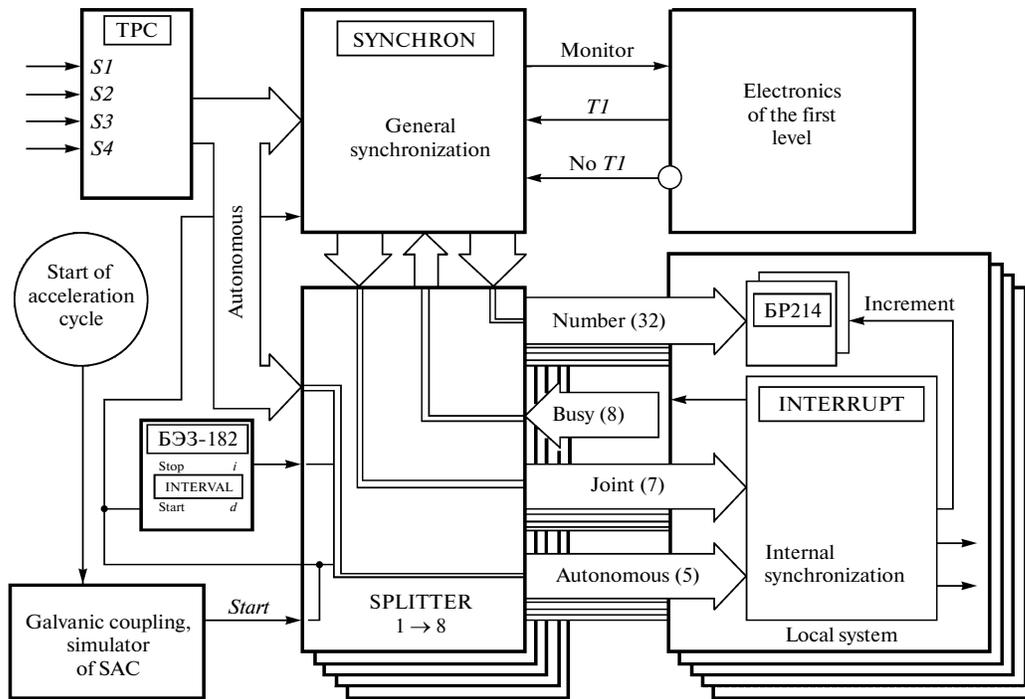The data are independently analyzed by the AAM modules, each channel of which, contains an ampli-

Fig. 14. Functional diagram of the synchronization system of the setup.

fier, three comparators, and a priority encoder and generates a two-bit word—the so-called channel status. The result of operation of each AAM module is a 16-bit word that contains information on the eight amplitude analysis channels and is sent to the output from the front panel of the module.

The two-bit status of each plate is derived by the TPM-2 module in the first-level RAM from the data of the status of each channel:

00—no particle (all segments are 00);

01—one particle (all segments are 00, and one segment is 01);

10—two particles (there is one segment with code 10 or two segments with codes 01);

11—three particles (there is one segment with code 11, or there is one segment with code 10 and the other with code 01, or there are two segments with codes 10, or there are three segments with codes 01).

The target status is produced in the second-level RAM from the status of each plate. The signals of the target status and the hodoscope state determine the state of the TPM-2 module output (whether $T1$ is true or false).

The main body of data was acquired with the trigger that required the presence of three or more particles in any of the five active target planes and two or more particles in the next plane, provided that two plates of the scintillation hodoscope were fired. Modules AAM had a dynamic range corresponding to five particles. The AAM thresholds were tuned to one, two, and

three particles, respectively. Events with a vertex in scintillator S_4 are filtered out by applying analog VETO to the signal from this scintillator. The tables stored in the TPM-2 and T-HOD modules in the form of text files containing a line-by-line address and a recorded datum were compiled using the LabView 4.0 package. These tables were entered into the memory of the modules only once upon starting the main data acquisition program. The decision making time from the instant of signal arrival at the input of the SYN-CHRON module to the instant of trigger production at the output of the TPM-2 module was 200 ns. The delay time from the instant of the particle hitting the target to the appearance of the trigger signal in the local DEGA system did not exceed 350 ns, which ensured synchronous operation of the γ detector.

Figure 13 presents the spatial distribution of vertices of interaction along the Z axis, which was obtained using tracks reconstructed in the precision vertex detector. Interactions both in silicon and in passive carbon and lead are clearly discernible in accordance with the material budget in these layers.

SVD-2 Synchronization System

The synchronization system is needed for coordinating the operation of all other systems in the setup. Its functional diagram is shown in Fig. 14. The system includes the TPC, SYNCHRON, INTERRUPT, БЭ3-182, and SPLITTER. In what follows, we present the purpose and functional features of each module.

The TPC module has been designed to process the signals arriving from the scintillation detectors of the primary trigger and has two sections—coincidence and veto. The veto section is designed on the K500TM131 IC. To reduce the influence of noise for the detectors included into the veto section, the module inputs responsible for these detectors are gated by the signal from the S_1 input. For the output signals of the primary trigger $T1.1$ and TRS, the delay time of the signal in the module is 16 ns, which can be attributed to the use of a 6-ns internal cable delay. The 8-bit trigger flag register is an important component of the module. It allows the coincidence signals of scintillation detectors, one of the frequencies of the generator nested in the module, and the signal of program-controlled start of the setup to be outputted or a signal from one of the supplementary inputs to be transmitted to the output.

Scintillation detectors S_3 and S_4 are fixed in place at the flange of the housing that covers the MSDs of the active target and the tracker part of the vertex detector, which guarantees their precise geometrical positions. The output signal from the PMT anode in S_4 was applied to the input of two pulse shapers. The threshold of the first shaper was adjusted so as to provide detection of a single particle, while the threshold of the second was raised with respect to the first to recognize interactions in the plastic. The output of the second pulse shaper was included in the veto section of the TPC module.

To reduce the effect of the scattered magnetic field on performance of PMTs in scintillation detectors, compensation coils were mounted on the housing of each PMT.

The SYNCHRON module located in the central crate of the Trigger local system performs the following tasks:

—receiving and transmitting the synchronization signals to the other local systems;

—triggering the data acquisition system of the active target, scintillation hodoscope, and Cherenkov detector;

—generating a 32-bit hardware code of the event number; and

—organizing service requests in the Trigger local system.

The event number counter is incremented by the trailing edge of the *Increment* pulse. The module receives the NIM signal *Start*; signals $C12$, CC, and $T1.1$ arriving from the TPC module; and enable signals from all local systems of the setup. This module is used to organize service requests in the Trigger local system. The module has the following registers: a request mask register, a request state register, an enable mask register, and a 32-bit event number counter. When the coincidence signal from triggered scintillation detectors arrives at the module's input, internal locking is set in it. This locking can be removed either

by the software after successful data transmission to the PC, or by hardware if the trigger signal of the first level is false. The delay time of this module for the *Monitor* signal is 40 ns.

The INTERRUPT module fulfills the functions similar to those of the SYNCHRON module in each local system. The INTERRUPT module has been designed for receiving and transmitting the synchronization signals and triggering the data acquisition systems, as well as for organizing service requests to the local computers, and outputting the enable signal that is transmitted to the Trigger local system. This module is capable of performing individual operations characteristic of this local system and is operable in either mode—autonomous or cooperative. Depending on its state, the module receives signals from one of the two groups. The autonomous mode is used to separately adjust data acquisition systems, and the cooperative mode is selected for data acquisition when it operates as part of the whole setup. The delay time of this module for the *Monitor* signal is 30 ns.

The БЭ3-182 module can be used as the delay unit in the range of $10^{-7}-10^2$ s and as a 10-bit counter with presets, or as a meander generator in three ranges (microsecond, millisecond, and second). In any of these ranges, the multiplier for the delay (or period) varies from 0.1 to 100. At its front panel, the module has the start input, the forced reset input, the delayed pulse output, and two outputs for an interval. All the inputs and outputs operate in the NIM levels. The module is not controlled over the CAMAC bus. In the synchronization system, it is used to organize various time gates and for monitoring the beam parameters.

A detailed description of the synchronization modules was presented in [48].

Sequence of the synchronization system operation. Let us assume that the system operates by the primary trigger signal from the scintillation detectors, local systems Trigger, Vertex, and Spectro operate in the full synchronization mode, while the local system DEGA operates in the partial synchronization mode (i.e., it receives only a fraction of all events). In this case, the event counter is zero.

The SYNCHRON module in the Trigger local system receives signal S (start) and distributes synchronized signal SS over all local systems. In this case, the hardware locking is introduced in each local data acquisition system, and the Trigger local system receives the *Busy* signal. The local computers of each system process the SS signal, removing the locking after the processing.

The SYNCHRON module in the Trigger local system receives signal CC or $T1.1$ and, within 40 ns, produces synchronized signal *Monitor* to switch on the electronics of the first level trigger $T1$. By signals *Monitor* and $T1$, the SYNCHRON module outputs signal *Increment*, which is transmitted to all local systems. In this case, the hardware locking is introduced in each
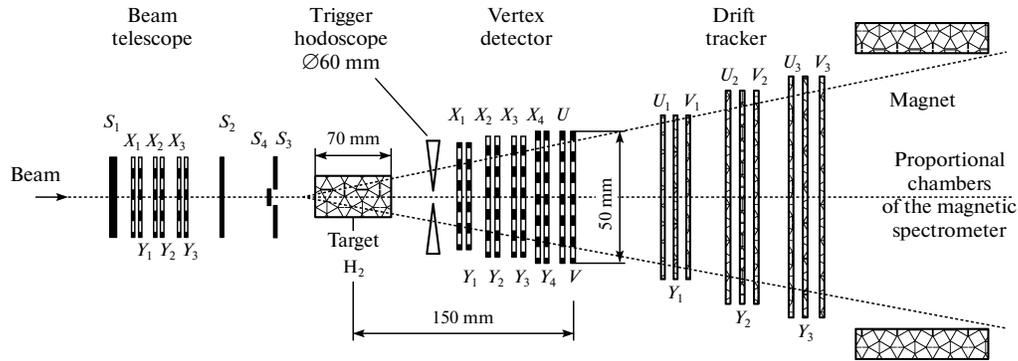
Fig. 15. Diagram of the setup header for the Thermalization project.

local data acquisition system and is transmitted to the Trigger local system. In response to the leading edge of the *Increment* signal, event numbers are written into the 32-bit registers in each local system. The 32-bit event counter in the SYNCHRON module is incremented by the trailing edge of the *Increment* signal. Note that the *Increment* signal may be delayed for different times with respect to the particle hit, depending on the trigger type.

If the DEGA local system operating in the partial synchronization mode did not have enough time to process the *Start* signal, it does not receive an event with zero number; nevertheless, the *Increment* signal makes a record into the event number register.

For the local computer, processing of an event consists in performing the following procedure:

(1) receiving and processing the request from the central crate;

(2) interrogating the event number register;

(3) interrogating crates and saving data to the hard or virtual disk; and

(4) removing the locking with the aid of the program.

During pauses between beam spills, the central computer Collector receives data from each local system over the Ethernet network, joins them according to the event number, and clears space on the disks of the local computers. At that time, receipt of the following events is disabled in the entire setup.

The SYNCHRON module and the INTERRUPT modules in the local systems prevent the passage of "cut" signals. During adjustment, the synchronization system allows independent operation of each local system.

THERMALIZATION PROJECT AT THE SVD-2 SETUP AND E-190 EXPERIMENT

Multiple production of particles at high energies is one of the fundamental problems in physics of hadrons. This process cannot be described in the strong interaction theory, since this theory provides only a qualitative pattern of a phenomenon: a hadron colli-

sion initiates a parton cascade. In the final phase of the parton cascade, when the energy of relative motion of partons is exhausted and the confinement forces become essential, partons join together, thereby forming hadrons. The mechanism of color retention (the confinement) has not yet been known. Therefore, it is impossible today to evaluate the basic characteristics of multiple production—the multiplicity distribution and the energy and mass spectra of particles.

The objective of the Thermalization Project at the SVD-2 setup [44], which was proposed in 2004 and numbered as SERP-E-190, is to study collective behavior of particles in the process of multiple production in *pp* interactions at proton beam energies $E = 50-70$ GeV. In the 1970s, the multiplicity distribution of particles was measured to charged particle number $n_{ch} = 16$ in the experiments on the Mirabelle bubble chamber at proton beam energy $E = 50$ GeV [49]. The mean number of charged particles is $\bar{n}_{ch} = 5.45$, the kinematical limit is $n_\pi = 58$, where n_π is the total number of charged and neutral pions. It was expected that events with total multiplicity $n = 20-40$ would be investigated. In this region, a large portion of the energy in the center-of-mass system is converted into the mass of secondary particles.

For the SVD-2 setup to be adapted for the tasks of this project, it was complemented with the following subsystems:

—a liquid-hydrogen target;

—an additional tracking system based on drift tubes; and

—a special trigger hodoscope for selection of high-multiplicity events.

The header of the modified setup is schematically shown in Fig. 15.

Liquid-Hydrogen Target

The liquid-hydrogen target is substituted for the active target at the vertex part of the setup. It has a diameter of 27 mm, a length of 70 mm, and a working volume of 37 mm³, which is filled with liquid hydrogen. The inner
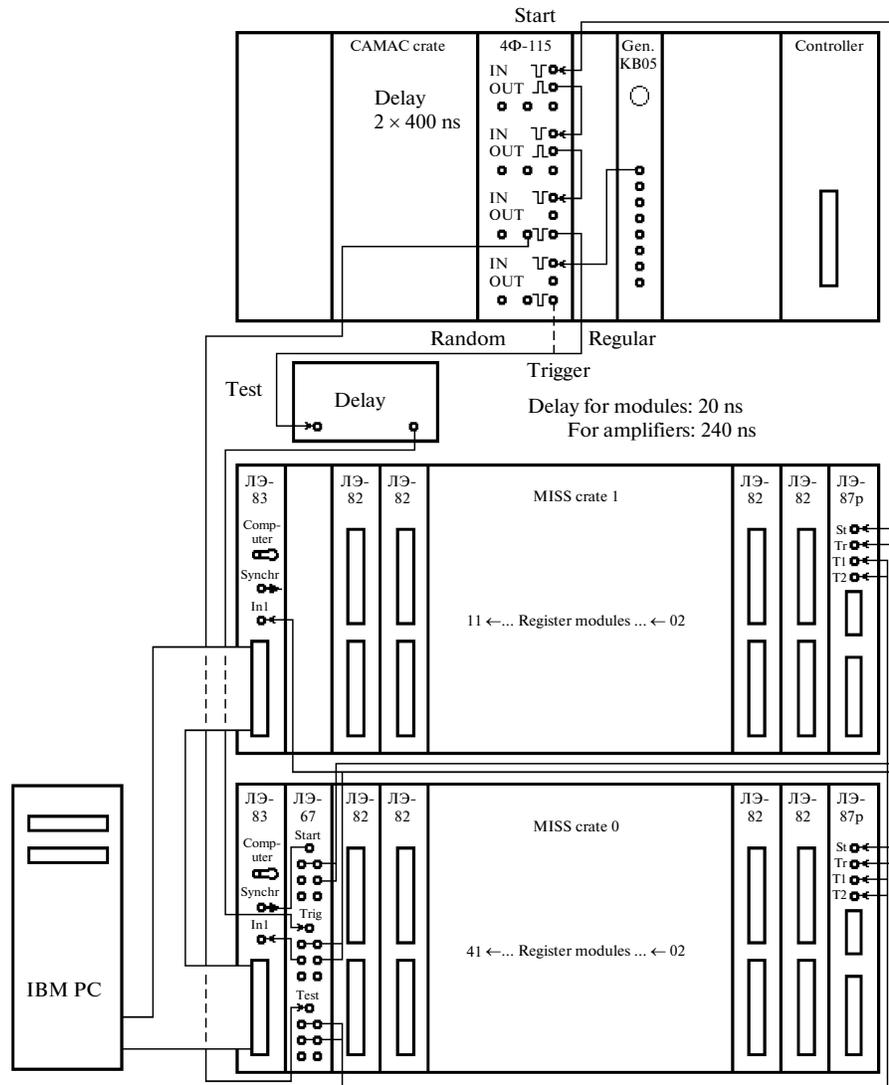
Fig. 16. Composition of the system for data taking from the drift tubes and intermodular connections.

vessel of the target is made from a 100-µm-thick Mylar film. A detailed description of the target design and its thermodynamic characteristics were presented in [50].

Tracking System

The tracking system is based on 2304 straw tubes, complements the silicon vertex detector, and allows precise reconstruction of multiparticle events and track extrapolation into the magnetic spectrometer. The system consists of three modules with dimensions (width × height) of 480×483, 700×771, and 900×1059 mm. These dimensions were selected so as to conform to the angular acceptance of the silicon vertex detector and the forward part of the magnetic spectrometer. Each module is composed of three chambers measuring particle coordinates X, U, and V. Chambers

of each module are identical, but the U and V detectors are located at angles of $\pm 10.5°$ with respect to axis Y. The modules are distributed downstream of the beam at a base of 950 mm. The chambers of each module are shifted downstream of the beam by 100 mm with respect to each other. Each chamber contains two layers of thin-walled drift tubes. The tube diameter $d = 6$ mm. To eliminate the left–right uncertainty in measuring the particle coordinates, the tubes of the first layer are displaced with respect to the tubes of the second layer by the radius value $d/2$. The walls of the tubes (the cathodes) are ~70 µm thick. Information is read out of the 30-µm-diameter anode wires. Each wire (tube) is an independent detection channel. The central zone with dimensions of 10×10 mm of each chamber is insensitive to beam particles. The accuracy in measuring the coordinate by the drift time is 150 µm. The
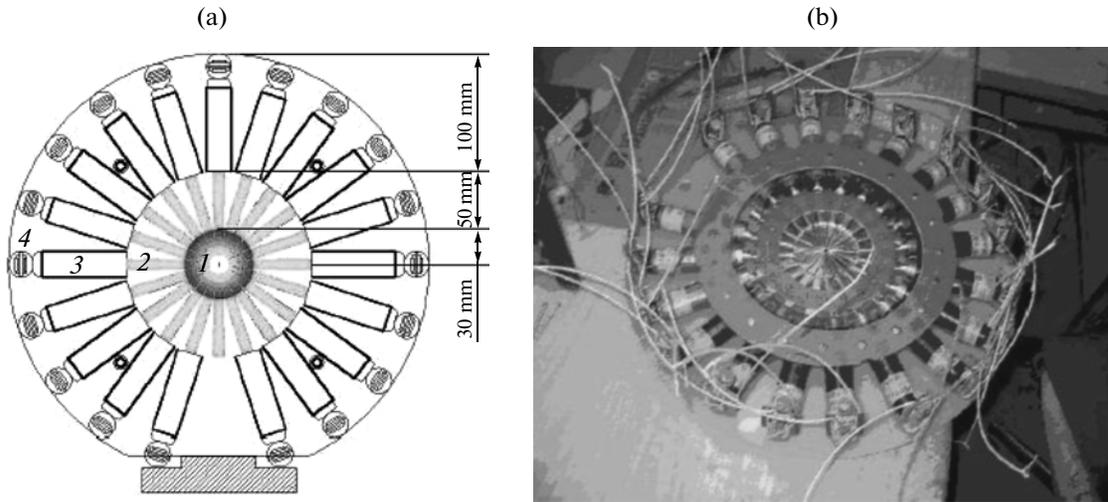
(a)   (b)

Fig. 17. (a) Composition of the trigger hodoscope: (*1*) scintillator, (*2*) light guide, (*3*) PMT, (*4*) voltage divider; and (b) trigger hodoscope being assembled.

two-track resolution is ~1.5 mm, the separation between the modules is ~150 mm, and the first module is located at a distance of 50 cm from the target.

Electronics of the straw tubes. The straw tubes have a total drift time of ~60 ns. The time-to-digital conversion modules developed for these detectors have a resolution of 2 ns, which allows one to obtain a coordinate resolution of ~0.15 mm.

The 32-channel shaping amplifiers for signal readout from the straw tubes [51] are based on the study [52]. The equipment for recording signals from the shaping amplifiers contains two MISS crates [42] for recording signals from straw tubes and one CAMAC crate for synchronizing the system performance [25] (Fig. 16). The MISS crates contain the following modules:

—64-channel ЛЭ-82 modules for multiple time-to-digital conversion (up to 5 starts in each channel, and the stop is common), the time resolution is 2 ns;

—the ЛЭ-83 crate controllers connected to the Q-bus communicating them to an IBM personal computer;

—special ЛЭ-87р modules for signal control and splitting; and

—ЛЭ-67 standard MISS splitters of the logical (NIM) signals.

There are ~150 words in each event. It is possible to receive data on ~1000 events in 1 s of beam extraction from the accelerator.

Trigger Hodoscope

The performance of the trigger subsystem in the E-190 experiment was described in detail in [53]. The signal for the occurrence of an event with a multiplicity higher than the predetermined threshold is obtained from analysis of signal amplitudes from the trigger scintillation hodoscope. The amplitudes are analyzed by AAM units. The trigger hodoscope (Fig. 17) is shaped as a chamomile with 19 petals—scintillators arranged to lie in the form of a disk 260 mm in diameter. The disk has a central hole 3.2 mm in diameter for beam guiding. BC-408 scintillator *1* is shaped as a truncated triangular plate with a height of 28 mm, a base of 8.6 mm, and a thickness of 1.8 mm. This plate is coated with a 6-μm-thick aluminized Mylar film to improve light collection. Organic glass light guide *2* is coupled to a petal and the entrance window of the ФЭУ-147-2 PMT by means of EPO301 optical epoxy resin [11]. Each PMT *3* is shielded from the external magnetic field (~50 G) with a 0.3-mm-thick μ-metal layer; the attenuation factor for this field is ~100.

At a proton beam intensity of $2 \times 10^6 \, \text{s}^{-1}$, the counting rate of a single petal due to charged particles escaping from the target is ~$10^3 \, \text{s}^{-1}$. The background particle flux incident on the trigger components is mainly caused by the beam halo, and its value is ~$2 \times 10^4 \, \text{s}^{-1}$ at optimum beam tuning. If the average anode current of the PMT is 0.1 mA and the high-current voltage divider is used, the permissible counting rate of the trigger element is $10^6 \, \text{s}^{-1}$. The high-voltage divider of the PMT has a resistance of 4.2 MΩ and an average current of 0.4 mA. The released heat power of a single detection channel is 0.8 W (the total hodoscope power is ~15 W), which does not exceed the permissible level of the electronics cooling system.

The dependence of the probability of trigger system activation on the number of tracks is shown in Fig. 18 for multiplicity thresholds $M = 3, 8, 12, 16, 20$, and 24 particles.
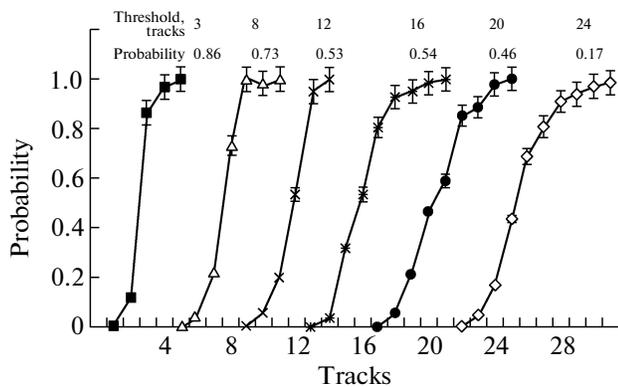
Fig. 18. Probability that the trigger will operate on the number of tracks in the hodoscope.

CONCLUSIONS

A number of important physical results have been obtained today owing to the high level of the SVD-2 spectrometer characteristics: the wide aperture, precision restoration of the vertex of interaction, possibility of reconstructing high-multiplicity events, and effective event selection. First and foremost, this is the study of open charm production in *pA* interactions at 70 GeV in the near-threshold region [54, 55], in which not only the integral cross section was measured, but also the differential cross sections of charm production. The topological measurements of the cross sections for multiple charged particle production in *pp* interactions at 50 GeV have been performed [56]. Thanks to the capabilities of the SVD-2 setup, the topological cross section has been measured for events with 24 charged particles in the final state, which are three orders of magnitude lower than the earlier values of the topological cross sections at this energy. The increase in the normalized variance $\omega^0 = \sigma^2(n_{\pi 0})/\langle n_{\pi 0}\rangle$ for neutral pions in events with particle multiplicity exceeding 22 has been detected for the first time at the SVD-2 setup [57]. This phenomenon may be the evidence of pion condensate production in events with a high multiplicity of particles in the final state.

It could seem that the setup should inevitably become obsolete and age over 20-year-long operation on the beam of the U-70 accelerator. Nevertheless, this has not happened, since the spectrometer with the vertex detector is consistently refined and upgraded. Over the past 8 years, almost all systems of the setup—the vertex detector with the related electronics, the tracker with its electronics, the γ detector with its electronics, and the trigger system—have been renewed. In the magnetic spectrometer, the power supplies have been replaced. The spectrometer electronics still remains on par with other systems in the data readout time and does not limit the data acquisition rate.

Of course, prior to starting each data acquisition session, the setup is carefully tested, and revealed failures are eliminated. As the experience of its operation

shows, computers are the components that most rapidly age and must be replaced first, power supplies are the next, and proportional chambers (anode wires burn out), together with their amplifiers, follow them.

Today, the SVD-2 setup is being prepared for a new experiment on studying anomalous soft photons in hadron−hadron interactions under the Thermalization Project.

REFERENCES

1. Andriishin, A.M., Ardashev, E.N., Babintsev, B.B., et al., *Preprint of Inst. for High Energy Phys.,* Serpukhov, 1984, no. 84-3.
2. Goldhaber, G., Pierre, F.M., Abrams, G.S., et al., *Phys. Rev. Lett.*, 1976, vol. 37, pp. 225−259.
3. Shindler, R.H., Alam, M.S., Boyarski, A.M., et al., *Phys. Rev. D,* 1981, vol. 24, pp. 78−97.
4. Baltay, C., Caroumbalis, D., French, H., et al., *Phys. Rev. Lett.*, 1978, vol. 41, pp. 73−79.
5. Alston, D., Cardman, L.S., Axel, P., et al., *Phys. Lett. B*, 1980, vol. 49, pp. 113−116.
6. Drijard, D., Clover, M.R., Cormier, T.M., et al., *Phys. Lett. B*, 1979, vol. 81, pp. 250−254; Drijard, D., Clover, M.R., Cormier, T.M., et al., *Phys. Lett. B,* 1979, vol. 85, pp. 452−457.
7. Giboni, K.L., Eisert, J., Wilkens, M., et al., *Phys. Lett. B*, 1979, vol. 85, pp. 437−442.
8. Basile, M., Romeo, G.R., Cifarelly, L., et al., *Nuovo Cimento A*, 1981, vol. 63, pp. 230−242.
9. Sandweiss J., Cardello, T., Cooper, P., et al., *Phys. Rev. Lett.*, 1980, vol. 44, pp. 1104−1107.
10. Bosetti, P., Bucksbaum, P., Chu, S., et al*., Phys. Lett. B*, 1979, vol. 74, pp. 343.
11. Church, M., Donaldson, R., Gustafson, R., et al., *Fermilab Proposal*, 1981, no. 690.
12. Asratyan, A.E., Epstein, V.Sh., Fakhrutdinov, R.M., et al., *Phys. Lett. B,* 1978, vol. 79, pp. 497−500.
13. Ardashev, E., Bogolyubsky, M., Bulgakov, N., et al., *Preprint of Inst. for High Energy Phys.*, Protvino, 1996, no. 96-98.
14. Ardashev, E.N., Boguslavsky, I.V., Gramenitsky, I.M., et al., *Nucl. Instrum. Methods Phys. Res. A,* 1995, vol. 356, pp. 210−219.
15. Basiladze, S.G., *Prib. Tekh. Eksp.*, 1983, no. 5, p. 6.
16. Basiladze, S.G., Smirnov, A.N., Stepanov, A.N., and Rybnikov, V.M., *Prib. Tekh. Eksp.*, 1985, no. 6, p. 68.
17. Baru, S.E., Basiladze, S.G., Groshev, V.R., et al., *Prib. Tekh. Eksp.*, 1975, no. 4, p. 105.
18. Belen'kii, V.Z., Bondar', N.F., Kazakov, I.B., et al., *Preprint of Leningr. Inst. of Nucl. Phys.*, Leningrad, 1985, no. 1049.
19. Basiladze, S.G. and Eloev, O.Z., 64 Channel Module for Signal Registration from RPC-213. Proportional

Chambers, in *Razrabotka apparatury sopryazheniya EVM s izmeritel'nymi ustanovkami* (Design of Devices for Connection of Computing Machines with Measurement Devices), Basiladze, S.G., Ed., Moscow: Mos. Gos. Univ., 1985.

20. Basiladze, S.G. and Eloev, O.Z., Specialized Controller for Data Selection and Reading from KPC Proportional Chambers, in *Razrabotka apparatury sopryazheniya EVM s izmeritel'nymi ustanovkami* (Designs of Devices for Connection of Computing Machines with Measurement Devices), Basiladze, S.G., Ed., Moscow: Mos. Gos. Univ., 1985.

21. Basiladze, S.G. and Rybnikov, V.M., *Prib. Tekh. Eksp.,* 1986, no. 1, p. 55.

22. Aleev, A.N., Basiladze, S.G., and Selikov, A.E., *Instrum. Exper. Techn.*, 2003, no. 5, pp. 624−627.

23. Basiladze, S.G., Smirnov, A.N., and Suvorov, V.V., *Prib. Tekh. Eksper.*, 1985, no. 1, p. 81.

24. Basiladze, S.G. and Rybnikov, V.M., Doubled Controlled 2BZU-122 Block of Delay, *in Apparatura sistem avtomatizatsii nauchnykh issledovanii MGU* (Devices of Scientific Study Automatization Systems), Moscow: Mod. Gos. Univ., 1984.

25. Bogdanova, G.A., Volkov, M.Yu., Leflat, A.K., et al., *Instrum. Exper. Techn.*, 2001, vol. 44, no. 4., pp. 449−454.

26. Ermolov, P.F., et al., *Proc. of 27th Int. Conf. on High Energy Physics. Glazgow, 1994*, Singapure: World Sci., 1995, p. 1029.

27. Avdeichikov, V.V., Aleev, A.N., Ardashev, E.N., et al., *Preprint of Inst. of Nucl. Phys. Mos. State Univ.*, Moscow, 1999, no. 99-27/585.

28. Avdeichikov, V.V., Aleev, A.N., Ardashev, E.N., et al., *Preprint of Inst. of Nucl. Phys. Mos. State Univ.*, Moscow, 1997, no. 97-40/49.

29. Ardashev, E.N., Bogolyubskii, M.Yu., Bulgakov, N.K., et al., *Preprint of Inst. of Nucl. Phys. Mos. State Univ.*, Moscow, 1999, no. 99-28/586.

30. Kartvelishvili, V.G., Likhoded, A.K., and Slabospitskii, S.R., *Yad. Fiz.,* 1981, vol. 33, no. 4, p. 832; Likhoded, A.K., Slabospitskii, S.R., and Suslov, M.V., *Yad. Fiz.*, 1983, vol. 38, p. 727.

31. Anjos, J.C., Herrera, G., Magnin, J., et al., *Preprint Centro Brasileiro de Pesquisas Fisicas*, 1997, no. NF-010/97; Anjos, J.C., Herrera, G., Magnin, J., et al., *Preprint Centro Brasileiro de Pesquisas Fisicas*, 1997, no. NF-011/97.

32. Alves, G.A., Amato, S., Anjos, J.C., et al., *Phys. Rev. Lett.,* 1993, vol. 70, pp. 722−725.

33. Verzocchi, M., *Nucl. Instrum. Methods Phys. Res. A,* 1994, vol. 351, pp. 222−224.

34. Frabetti, P.L., Bogart, C.W., Cheung, H.W.K., et al., *Phys. Rev. Lett. B.*, 1990, vol. 251, pp. 639−644.

35. Blümlein, J., Brunner, J., Grabosch, H.-J., et al., *Phys. Rev. Lett. B*, 1992, vol. 279, pp. 405−410.

36. Basiladze, S.G., Bogdanova, G.A., Volkov, V.Yu., et al., *Instrum. Exper. Techn.*, 2006, vol. 49, no. 3, pp. 350−357.

37. Ardashev, E.N., Basiladze, S.G., Bogdanova, G.A., et al., *Instrum. Exper. Techn.*, 2007, vol. 50, no. 5, pp. 646−663.

38. Ardashev, E.N., Babintsev, V.V., Vorob'ev, A.P., et al., *Preprint of Inst. for High Energy Phys.,* Protvino, 2001, no. 2001-31.

39. Santiard J.C., Beusch W., Buytaert, S., et al., *Preprint of CERN*, 1994, no. ECP/94-17.

40. Ansel, P., Boulter, R., Czermak, A., et al., *Nucl. Instrum. Methods Phys. Res. A,* 1992, vol. 315, pp. 425−429.

41. Le Croy Catalog, December 1982, USA.

42. Bushnin, Yu.B., Van'ev, V.S., Goncharov, P.I., et al., *Preprint of Inst. for High Energy Phys.*, Serpukhov, 1988, no. 88-47.

43. Ardashev, E.N., Bogdanova, G.A., Volkov, V.Yu., et al., *Preprint of Inst. of Nucl. Phys. Mos. State Univ.* Moscow, 2005, no. 14/780.

44. Avdeichikov, V.V., Aleev, A.I., Balandin, V.P., et al., *Soobshchenie OIYaI* (Report of Joint Inst. for Nucl. Res.), Dubna, 2004, no. P1-2004-190.

45. Deryugin, O.A., Zverev, E.G., and Leflat, A.K., *Instrum. Exper. Techn.,* 1998, vol. 41, no. 1, pp. 63−67.

46. Ermolov, P.F., Zverev, E.G., Karmanov, D.E., et al., *Instrum. Exper. Techn.*, 2002, vol. 45, no. 2, pp. 194−206.

47. Bogdanova, G.A., Bogolyubskii, M.Yu., Volkov, V.Yu., et al., *Soobshchenie OIYaI* (Report of Joint Inst. for Nucl. Res.), Dubna, 1995, no. P1-95-451.

48. Bogdanova, G.A., Volkov, V.Yu., Leflat, A.K., et al., *Preprint of Inst. of Nucl. Phys. Mos. State Univ.*, Moscow, 2000, no. 2000-25/629.

49. Ammosov, V.V., Boitsov, V.N., Ermolov, P.F., et al., *Phys. Lett. B*, 1972, vol. 42, pp. 519−521.

50. Borzunov, Yu.T., Golovanov, L.B., Kireev, V.I., et al., *Preprint of Inst. for High Energy Phys.*, Protvino, 2009, no. 2009-4.

51. Basiladze, S.G., Baturitskii, M.A., Bogdanova, G.A., et al., *Instrum. Exper. Techn.*, 2008, vo. 51, no. 3, pp. 336−341.

52. Baturitsky, M.A. and Dvornikov, O.V., *Nucl. Instrum. Methods Phys. Res. A,* 1999, vol. 423, pp. 163−173.

53. Avdeichikov, V.V., Bogdanova, G.A., Budilov, V.A., et al., *Instrum. Exper. Techn.*, 2011, vol. 54, no. 2, pp. 159−168.

54. Ryadovikov, V.N., et al., *Phys. At. Nuclei*, 2010, vol. 73, pp. 1539−1550.

55. Ryadovikov, V.N., et al., *Phys. At. Nuclei*, 2011, vol. 74, pp. 324−331.

56. Ardashev, E.N., Bogolyubskii, M.Yu., Bulgakov, N.K., et al., *Preprint of Inst. for High Energy Phys.*, Protvino, 2011, no. 2011-4. arXiv [hep-ex] 1104.0101

57. Ardashev, E.N., Bogolyubskii, M.Yu., Bulgakov, N.K., et al., *Preprint of Inst. for High Energy Phys.*, Protvino, 2011, no. 2011-5. arXiv [hep-ex] 1104.3673.